Magmatism in the Asunción-Sapucai-Villarrica graben (Eastern Paraguay) revisited.
Petrological, geophysical, geochemical and geodynamic inferences

Piero Comin-Chiaramonti[a,e], Angelo De Min[a], Aldo Cundari[b], Vicente A.V. Girardi[c],
Marcia Ernesto[d], Celso B. Gomes[c], Claudio Riccomini[c]

[a]*Geosciences Department, Trieste University: Via Weiss 8. I-34127 Trieste, Italy*
[b]*Geotrack International Pty Ltd, P.O. Box 4120, Melbourne, Victoria 3052, Australia*
[c]*Geosciences Institute, University of São Paulo, Cidade Universitária, Rua do Lago, 562, 05508-900 São Paulo, Brazil.*
[d]*Astronomic and Geophysic Institute (IAG) of the São Paulo University, Brazil.*
[e]*Corresponding author: e-mail:* comin@univ.trieste.it

Abstract

The Asunción-Sapucai-Villarrica graben (ASV) in Eastern Paraguay at the westernmost part of the Paraná Basin, was the site of intense magmatic activity in Mesozoic and Tertiary times. During the Early Cretaceous, tholeiitic and K-alkaline magmatism predated the Paleocene-Oligocene alkaline sodic magmatism. Geological, petrological, mineralogical and geochemical results, based on a synthesis of previous studies, indicate that the following magmatic events are dominant in the area: 1) tholeiitic basalt and basaltic andesites, flows and sills (Serra Geral Formation) of low- and high-titanium types; (2) K-alkaline magmatism, where two suites are distinguished, i.e. basanite to phonolite (B-P) and alkali basalt to trachyte (AB-T), and their intrusive analogues; (3) ankaratrite to phonolite with strong Na-alkaline affinity, where the mantle xenoliths in ultramafic rocks are also present in two suites, i.e. high- (HK) and low-potassium (LK), respectively. ASV structural and geophysical data show extensional characteristics. The tholeiitic and potassic rocks have geochemical features characterized by negative Ta-Nb and positive Ba-Sm spikes; on the other hand the patterns of the ASV sodic rocks are distinct for their positive Ta-Nb and negative K-Sm spikes. This implies different mantle sources, consistently with Sr-Nd isotopes that are Rb-Nd enriched and depleted for the potassic and sodic rocks, respectively. Nd model ages suggest that some notional distinct "metasomatic events" may have occurred during Paleoproterozoic to Neoproterozoic times as precursor to the alkaline and tholeiitic magmas. It seems, therefore, that the genesis of the ASV magmatism is dominated by a lithospheric mantle, characterized by small-scale heterogeneity.

Key words: Asunción-Sapucai-Villarrica graben, Paraguay, tholeiitic and alkaline magmatism, mantle xenoliths, geophysical and geochemical characteristics, geodynamic implications.

1. Introduction

Velázquez et al. (2011) presented a structural analysis of the "central segment of the "Asunción Rift", mainly based on the previous papers related to the Eastern Paraguay magmatism in general, and to the Asunción-Sapucai-Villarrica graben (ASV) in particular, and also counting on a large amount of field work data collected last years on the dyke-swarms cropping out in the area. However, some aspects, as e.g. the close association in space of potassic and sodic alkaline rock-types with tholeiitic dykes and flows (both of high- and low-Ti types; cf. Bellieni et al. 1986a), have not been subject of a more detailed discussion by those authors.

This paper seeks to evaluate geological, petrological, geophysical and geochemical data on the magmatism from the western margin of the Paraná-Angola-Etendeka System (PAE), where tholeiitic flows and dykes (Early Cretaceous, both of high-Ti and low-Ti types; cf. Fig. 1A and Piccirillo and Melfi, 1988) are associated in time and space with a wide variety of alkaline rock-types (both potassic and sodic) and carbonatites. The investigated alkaline and tholeiitic rocks from Eastern Paraguay span in age mainly from Early Cretaceous to Paleogene times. Therefore, they are germane to the magmatic and tectonic evolution of the PAE and of the Atlantic Ocean (cf. Fig 1 B and Comin-Chiaramonti et al., 2007a,b).

Finally, it should be stressed that the present paper represents a synthetic review of the previous investigations done by a group of researchers from Italy and Brazil, coordinated by Comin-Chiaramonti and C.B. Gomes since 1981 and 1986, respectively.
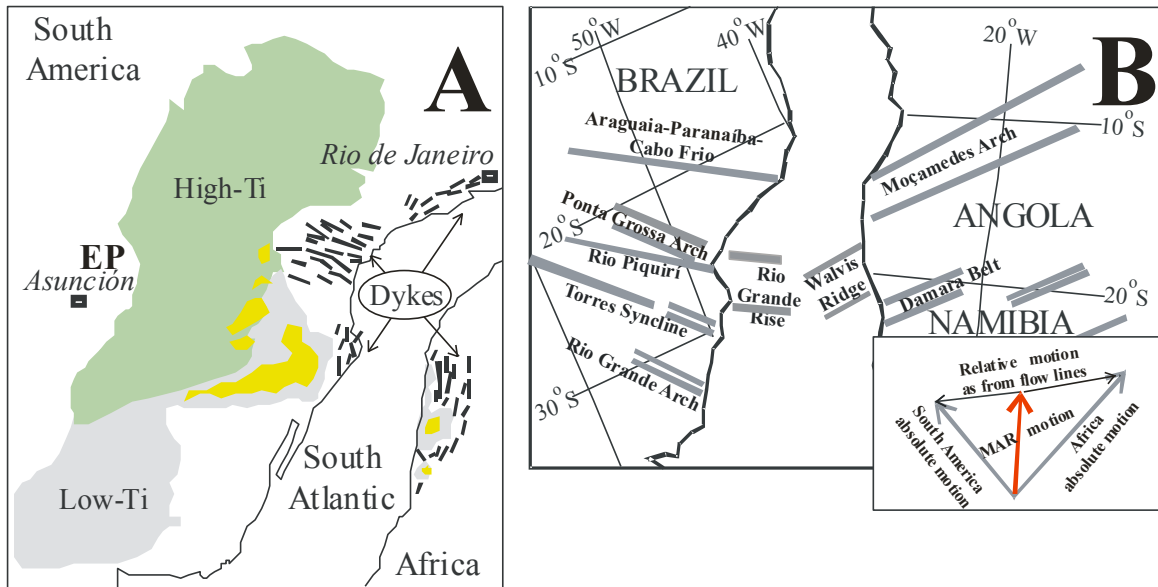
Fig. 1. A. Sketch map of the Paraná-Angola-Etendeka system (Piccirillo and Melfi, 1988), where the arrows indicate the occurrences of the main dyke-swarms. The basaltic lavas are subdivided into broad high- and low-Ti groups, and late-stage rhyolites (yellow fields). EP: Eastern Paraguay. **B**. Main lineaments in the Paraná-Angola-Etendeka System (PAE), western Gondwana at ca. 110 Ma (modified after Comin-Chiaramonti et al., 2011), corresponding to the main lineaments of the alkaline and alkaline-carbonatitic complex. Inset: vector diagram showing relationships among absolute plate motions, relative motions, and motion of the Mid Atlantic Ridge (MAR, after Fairhead and Wilson, 2005).

2. Eastern Paraguay: geological outlines and geophysical evidences

Eastern Paraguay shows a complex block-faulted structure between the southern Precambrian tip of the Amazonian Craton (Apa block) and the northern one of the Rio de la Plata Craton (Caacupú high; Fig. 2). This intercratonic area, including the westernmost fringe of the Paraná Basin (PB), represents an undeformed basin at the western Gondwana (Fig.1), where the sedimentation, started in Cambrian times, was topped by Early Cretaceous tholeiitic basalts of the Serra Geral Formation (Zalán et al., 1990; Roger et al., 1995), and followed by younger sedimentation (Fig. 2).

Moreover, it should be also noted that Eastern Paraguay lies along the former western margin of the Gondwana, bounded by an anticlinal structure established since Early Paleozoic, the Asunción Arch, that separates the Paraná Basin (East) from the Gran Chaco Basin (West) (Comin-Chiaramonti et al., 1997). PB shows a high-velocity upper-mantle lid with a maximum S-wave velocity of 4.7 km/s (Moho 37 km depth), with no resolved low-velocity zone to at least a depth of 200 km (Feng et al., 2007). Betweeen the two blocks, i.e. Apa and Caacupú of Fig. 2, Eastern Paraguay was subjected to NE-SW-trending crustal extension during Late Jurassic-Early Cretaceous, probably related to the western Gondwana break up (Fig. 1; Comin-Chiaramonti et al., 1997, 1999 and therein references). NW-SE fault trends, paralleling the dominant orientation of Mesozoic alkaline and tholeiitic dykes, reflect this type of structure (Comin-Chiaramonti et al., 1992a, Riccomini et al., 2001).

From the aereomagnetic survey (Anschutz, 1981, Druecker and Gay, 1987), the linear magnetic anomalies trend mainly N40-45W (Fig. 3). These anomalies have been interpreted as reflecting Early Cretaceous tholeiitic dyke-swarms (Druecker and Gay, 1987), but field evidence does not support this hipothesis. It seems possible that most magnetic anomalies correspond to older Precambrian tectonic lineament (Ussami et al., 1994). The Landsat lineaments, trending mainly NE and E-W, would reflect tectonic lineaments of the basement (De Graff, 1985).

The Bouguer gravity map (Fig. 3) consists of prevailing NW-trending gravity "highs" and "lows" that represent shallow to exposed basement and sedimentary basins, respectively (Photo

Gravity Co., 1986): the boundaries between gravity highs and lows are generally marked by step gradients that reflect abrupt basement offsets along faults, or basement dip changes by crustal warping. Notably, the gravity lows and highs parallel the dominant NW attitude of the magnetic lineaments, with post-Paleozoic magmatism (both tholeiitic and alkaline) associated with gravity lows. In this context the ASV represents the most important geological structure of the region (see later).
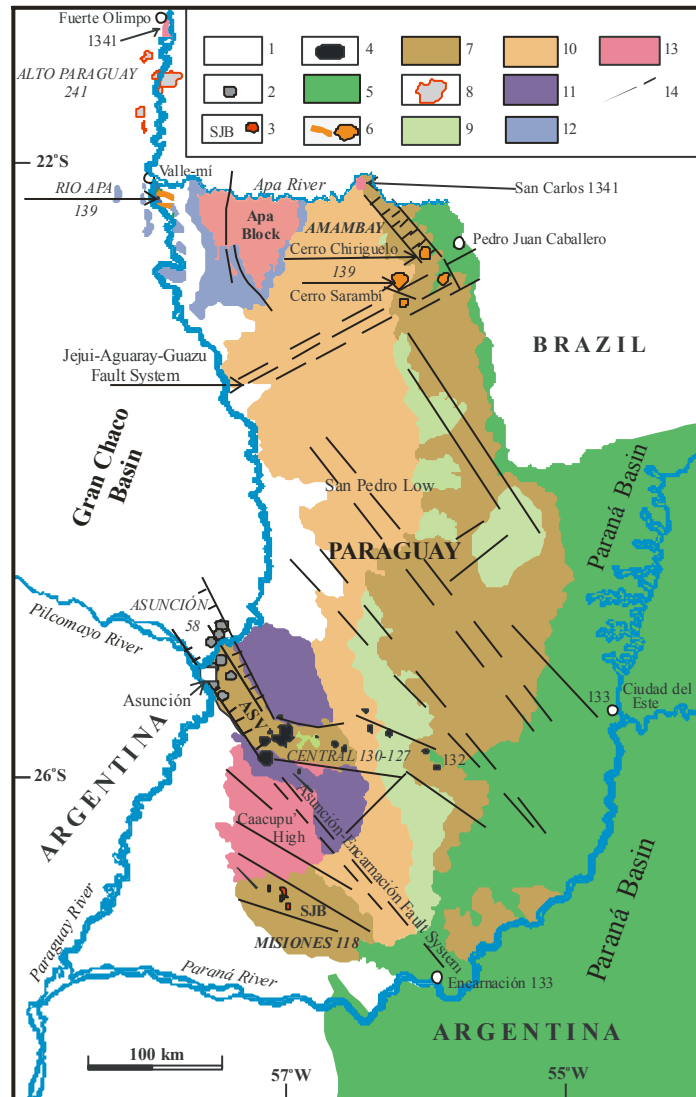
Fig. 2. Geological sketch-map of Eastern Paraguay (modified after Hutchinson, 1979; Wiens, 1982; Livieres and Quade, 1987; Kanzler, 1987; Comin-Chiaramonti et al., 1992a, 1997; Comin-Chiaramonti and Gomes, 1996). ASV: Asunción-Sapucai-Villarrica graben. 1: Neogene and Paleogene sedimentary cover (e.g. Gran Chaco); 2: Paleogene sodic alkaline rocks, Asunción Province; 3: Late Early Cretaceous sodic alkaline rocks (Misiones Province, San Juan Bautista, SJB); 4: Early Cretaceous potassic alkaline rocks (post-tholeiites; ASU: Asunción-Sapucai-Villarica graben, Central Province); 5: Early Cretaceous tholeiites of the Paraná Basin (Serra Geral Formation in Brazil and Alto Paraná Formation in Paraguay: cf. Comin-Chiaramonti et al., 2007a); 6: Early Cretaceous potassic alkaline rocks (pre-tholeiites, Apa and Amambay Provinces); 7: Jurassic-Cretaceous sedimentary rocks (Misiones Formation); 8: Permo-Triassic alkaline rocks (Alto Paraguay Province); 9: Permian sedimentary rocks (Independencia Group); 10: Permo-Carboniferous sedimentary rocks (Coronel Oviedo Group); 11: Ordovician-Silurian sedimentary rocks (Caacupé and Itacurubí Groups); 12: Cambro-Ordovician platform carbonates (Itacupumí Group); 13: Archean to Early Paleozoic crystalline basement: high- to low-grade metasedimentary rocks, metarhyolites and granitic intrusions; 14: major tectonic lineaments and faults. The radiometric values, e.g. 133 Ma are referred to $^{40}Ar/^{39}Ar$ plateau ages for the main magmatic types (Renne et al., 1992, 1993, 1996) and to Rb/Sr ages for the Precambrian rhyolitic rocks of Fuerte Olimpo and Fuerte San Carlos (Gomes et al., 2000).
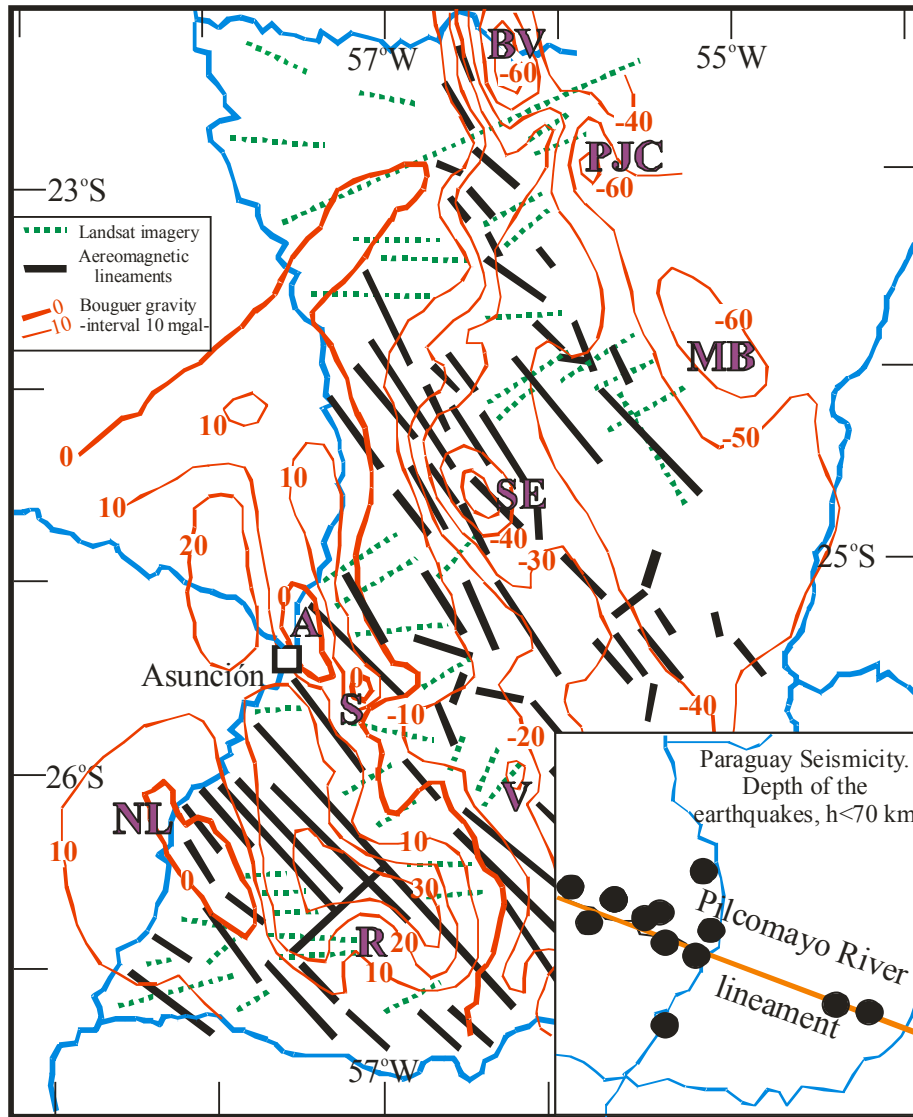
Fig. 3. Geological sketch-map showing aereomagnetic and Landsat lineaments in Eastern Paraguay, and Bouguer gravity data (De Graff, 1985; Drueker and Gay, 1987; Ussami et al., 1994). Gravity lows: BV, Bella Vista; PJC, Pedro Juan Caballero; MB, Mbacarayú; SE, San Estanislao (formely San Pedro); A, Asunción, S, Sapucai, V, Villarrica (ASV graben); R, Santa Rosa. **Inset**: distribution of earthquakes with depth < 70 km (Berrocal and Fernandes, 1996).

Finally, it should be noted that the present seismic activity (earthquakes with deep <70 km) indicates that the NW-trending fault systems continue up to present day, i.e. the Pilcomayo lineament: (inset of Fig. 3), that can be considered to be aligned with the Piquirí lineament and the Torres syncline (Fig. 1B).

In conclusion, the resulting structural pattern controlled the development of grabens or semigrabens as a response to NE-SW-directed extension and continued evolving into Cenozoic times (Comin-Chiaramonti and Gomes, 1996, Comin-Chiaramonti et al., 1999). According to Tommasi and Vauchez (2001), rift orientations seem to have been controlled by the pre-existing lithospheric mantle fabric, as indicated by deep geophysical data.

The thermal history, using apatite fission track analyses (AFTA), reveals that at least two main episodes have been identified in sedimentary and igneous/metamorphic samples ranging in age from Late Ordovician to Early Cretaceous (Green et al., 1991, Hegarty et al., 1996). AFTA data from ASV show evidence for rapid cooling beginning some time between 90 and 80 Ma, similar to the results found along Brazilian and Uruguayan coasts. A Tertiary heating/cooling episode is also suggested by AFTA data (60-10 Ma), supporting early work in the area. The time of the first event

is significantly younger than any rifting activity related to the Paraná flood basalts and to the opening of the South Atlantic. Late Cretaceous cooling may have involved several kilometers of differential uplift and erosion, and would have played an important role in the control of the geomorphology and drainage patterns of the region, especially in the ASV system (Green et al., 1991, Hegarty et al., 1996).

In summary, from the field stratigraphic control and starting from Mesozoic times (Fig. 2), almost five main alkaline magmatic events have occurred in Eastern Paraguay, other than the Early Cretaceous tholeiitic magmatism (133-134 Ma; Comin-Chiaramonti et al., 2007a). Three of them include rocks of sodic affinity, corresponding geographically to the provinces of Alto Paraguay (241.5±1.3 Ma), Misiones (118.3±1.6 Ma) and Asunción (58.7±2.4 Ma), whereas two involve rocks of potassic affinity associated with the Apa and Amambay provinces, both of similar age (138.9±0.7), and with the Central Province (ASV, 126.4±0.4 Ma).

3. Asunción-Sapucai-Villarrica graben (ASV)

The ASV graben (Fig. 4) is the most apparent rifting structure in Eastern Paraguay, linked to NE-SW extensional vectors (Comin-Chiaramonti et al., 1992a), and it is characterized by a gravity anomaly trending N30-45W near Asunción townships (Fig. 3). The graben, nearly symmetrical and defined by major faults along each margin (De Graff, 1985; De Graff et al., 1981; Comin-Chiaramonti et al., 1999; Velázquez et al., 2011), can be subdivided into three main segments (Fig. 4): 1) the northwestern part, between the Asunción and Paraguarí townships, indicated also by the intragraben Ypacaray rifting and by the presence of Na-alkaline mafic-ultramafic plugs carrying mantle xenoliths (Asunción Province; age between 66 and 39 Ma; cf Fig. 4); 2) a central area, defined between Paraguarí and La Colmena townships, characterized by K-alkaline complexes and dykes (averaged age 127 Ma; cf Figs. 3) and 4), and by subordinate Na-alkaline complexes and dykes (age around 66-60 Ma); 3) the eastern part, between La Colmena and the Ybytyruzú hills, characterized by K-alkaline complexes and dykes (age around 130-125 Ma) and by tholeiitic lavas and flows (age around 133-130 Ma; cf. Comin-Chiaramonti et al., 2007a).

Geology and gravity results indicate that the ASV graben extends up to 100 km into the Chaco Basin (Figs. 2 and 3), and turns to a N80W trend between Paraguarí and Villarrica townships, in the area marked by a gravity low anomaly that increases eastwards (Figs. 3 and 4). Paleomagnetic data by Ernesto et al. (1996) revealed that the potassic Cretaceous rocks (75 samples) have reversal polarity remnants corresponding to a paleomagnetic pole at 62.3°E and 85.4°S, similar to that calculated for the Serral Geral Formation in the Paraná Basin. It is inferred that ASV K-alkaline rocks were emplaced while the tholeiitic magmatic activity was still taking place (Fig. 1).

It should be also noted that the Tertiary sodic rocks, carrying mantle xenoliths, mainly occur in an area characterized by relatively gravity highs (Fig. 3), whereas the potassic complexes and dykes occur in a gravity low belt characterized by block faulting (Figs. 3 and 4). Finally, at East of the city of Villarrica, a NS-trending fault system bounds the western side of the Ybytyruzú hills, close to several alkaline intrusions (Comin-Chiaramonti and Gomes, 1996).

A total of 527 samples from the ASV area, including 220 dykes, have been investigated in detail, being the data on field geology, age, orientation (dykes), petrography and mineral chemistry of the rocks available in Comin-Chiaramonti et al. (1992a, 1996a, b, c, d, 1997). In particular 55% of the dykes are preferentially oriented N20-60 W, as shown e.g. for the B-P and AB-T dykes (Fig. 5, III).

ASUNCIÓN-SAPUCAI-VILLARRICA GRABEN

N

km

0   10   20

Legend:

- Tertiary-Quaternary sediments
- Early Cretaceous tholeitic basalts (Alto Parana' F.)
- Triassic-Jurassic continental sediments
- Carboniferous and Permian continental sediments
- Late Ordovician-Early Silurian continental sediments
- Cambrian-Ordovician crystalline basement

- Tertiary Na-alkaline complexes and dykes
- Early Cretaceous K-alkaline complexes and dykes
- Major faults

CHACO

Asunción

Paraguay River

Ypacaraí Valley

Yaguarón

Paraguarí

Carapeguá

Acahay

Ybycuí

La Colmena

Villarrica

Caballero

Sapucai

Ybytyruzú Hills

Fig. 4. Geological sketch-map of the Asunción-Sapucai-Villarrica graben showing the main occurrences of magmatic rock-types, modified after Comin-Chiaramonti et al. (1996a). In parentheses preferred K/Ar and plateau Ar/Ar ages (in bold) in Ma according to Comin-Chiaramonti et al. (1996a and 2007a, respectively). *K-alkaline complexes*: 1, Cerro Km 23 (132, **128**); 2, Cerro San Benito (**127**); 3, Cerro E. Santa Elena (**126**); 4, Northwestern Ybytyruzú (125-129); 5, Cerro Capiitindy (n.a.); 6, Mbocayaty (126-130, **126**); 7, Aguapety Portón (128-133, **126**); 8, Cerro Itapé (n.a.); 9, Cerrito Itapé (n.a.); 10, Cerro Cañada (**127**); 11, Cerro Chobí (n.a.); 12, Potrero Garay (n.a.); 13, Catalán (n.a.); 14, Cerro San José (**127**); 15, Potrero Ybaté (126-128, **128**); 16, Sapucai (119-131, **126**); 17, Cerro Santo Tomás (126-130, **127**); 18, Cerro Porteño (n.a.); 19, Cerro Acahay (118, **127**); 20, Cerro Pinto (n.a.); 21, Cerro Ybypyté (124); 22, Cerro Arrúa-í (126-132, **129**). *Na-alkaline complexes*: A, Cerro Patiño (39); B, Limpio (50); C, Cerro Verde (57, **61**); D, Ñemby (46, **61**); E, Cerro Confuso (55-61); F, Nueva Teblada (46-57); G, Lambaré (49); H, Tacumbú (41-46, **58**); I, Cerro Yarigua-á (n.a.); J, Cerrito (**56**); K, Cerro Gimenez (66); L, Cerro Medina (n.a.); M, Colonia Vega (n.a.). Detailed information on the single occurrences, i.e. geological map, location, country rocks, forms and main rock-types are provided in Comin-Chiaramonti et al. (1996a, b, c, d); n.a. not available.

4. Classification, petrography and petrochemistry of the magmatic rocks

The fine-grained texture of the ASV rocks, including the intrusive variants, are plotted on the De La Roche (1986) chemical classification (Fig. 5), with an additional subdivision based on the K_2O and Na_2O wt% contents displayed on the Le Maitre's (1989) diagram (inset I). Judging from the data 4% of the dykes have tholeiitic affinity (sills, lava flows, and dykes, both high- and low-Ti variants, according to Bellieni et al., 1986a, b), and straddles the fields of the olivine tholeiitic basalts and andesibasalts, whereas 17% are sodic and 79% potassic in composition. The distribution of the potassic rocks shows that the variation of the dykes is consistent with that of the associated intrusive and volcanic rocks (inset I). Two main lineages are apparent for the potassic rock-types (Fig. 5 and inset II): 1) a silica undersatured lineage (B-P) ranging from basanite to phonolite and peralkaline phonolite, and 2) a silica-saturated lineage (AB-T) ranging from alkali basalt to trachyphonolite and trachyte (Gomes et al., 1989; Comin-Chiaramonti et al., 1992a, 1993).

In conclusion, in a relatively narrow area represented by ASV graben (ca. 35x200 km, cf. Fig. 3) tholeiitic rock-types (both high-titanium, H-Ti, and low-titanium, L-Ti, variants), K-alkaline and Na-alkaline rocks are widespread. In Tables 1 to 4 representative and average analyses of these rocks are reported.

4.1. Tholeiites

The tholeiitic rocks are mainly lava flows (Ybytyruzú hills) and doleritic sills occurring usually near the Ybycuí township (Fig. 4). The textures are porphyritic to hyalophitic (lava flows and dykes) and doleritic (sills), characterized by the presence of two clinopyroxenes (augite and pigeonite), and by pronounced variations of TiO_2 (1.4 to 3.2 wt%; cf. Table 1) and incompatible element contents (e.g., Ba ca. 150 to 400 ppm, Zr ca. 100 to 200 ppm). These variations are similar to those common to tholeiitic basalts of the Paraná Basin that are dominated by low and high contents of TiO_2 (L-Ti and H-Ti variants: southern and northern Paraná Basin with TiO_2 <2 and >2.5 wt%, respectively; cf. Fig. 1), and incompatible elements (Bellieni et al., 1987; Piccirillo et al., 1988). The mineral assemblages (augite, pigeonite, olivine, plagioclase, magnetite, ilmenite) show crystallization temperatures around 1200-1000°C and fO_2 conditions between NNO and QMF buffers (Bellieni et al., 1987; Piccirillo and Melfi, 1988).

Mass balance calculations and the remarkable differences in incompatibile element ratios between L-Ti and H-Ti tholeiites suggest that such differences cannot be explained by fractional crystallization, or by means of melting and zone refining processes of a homogeneous mantle source. A basalt genesis from chemically different lithospheric mantle materials is therefore proposed, expecially considering that mixing processes seem to have played a minor role (Bellieni et al., 1986a, b; Piccirillo et al., 1989).
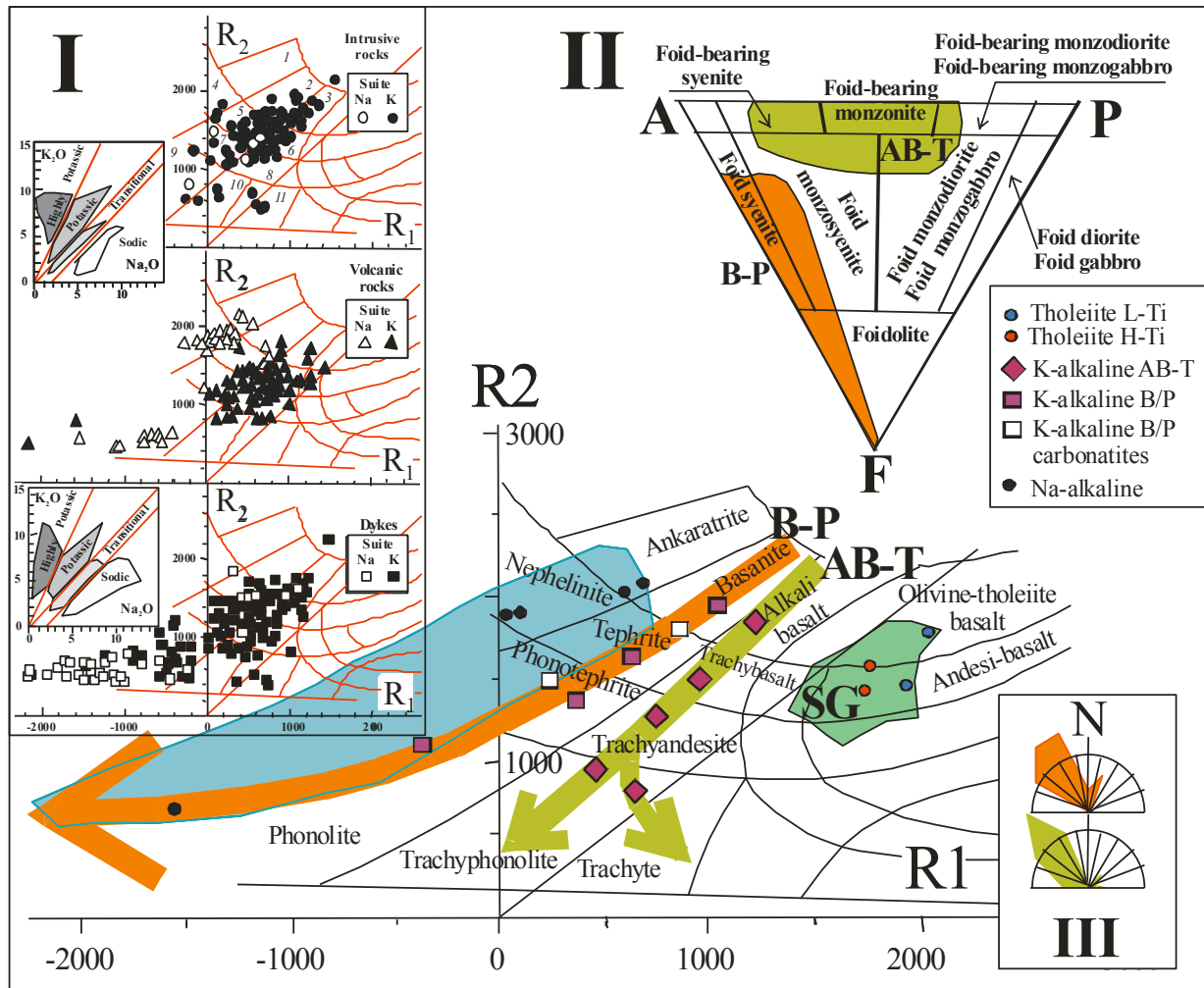
Fig. 5. Compositional variation of the rock-types from ASV in terms of R1=4Si-11(Na+K)-2 (Fe+Ti) and R2=6Ca+Mg+Al (De La Roche, 1986; cf. also Fig. 2 of Comin-Chiaramonti et al., 1992a). Data source: Comin-Chiaramonti et al. (1996b). SG, field of Serra Geral tholeiites; ASV, field of Na-alkaline rocks; B-P and AB-T, lineages of the K-alkaline rocks (basanite to phonolitic suite and alkaline basalt to trachyphonolite/trachyte suite, respectively; white squares represent a lava flow and a theralite with carbonatitic affinity, respectively (see text). Insets: **I**, the same with subdivision into intrusive and volcanic rocks and dykes, plus Le Maitre (1989) classification, as in Fig. 2 of Comin-Chiaramonti et al. (1997). **II**, QAPF diagram (Streckeisen, 1979) for intrusive potassic suites from ASV, as from Fig. 3 of Comin-Chiaramonti et al. (1997). **III**, Azimutal frequence of the B-P and AB-T dykes (Gomes et al., 1989). The symbols represent selected compositions as in Tables 1 to 4.

4.2. Potassic suites

Based on Fig. 5 and Tables 2 and 3, these reporting representative analyses of different lithotypes), the potassic rocks are subdivided in B-P and AB-T lineages, a distinction also confirmed by crystal fractionation models (Comin-Chiaramonti et al., 1992a). Chemical analyses of the coexisting mineral phases are listed in Comin-Chiaramonti et al. (1992a).

B-P suite. The effusive rock-types and dykes (basanites, tephrites and phonotephrites) show typically porphyritic textures with phenocrysts of clinopyroxene ($Wo_{40-50}Fs_{10-19}$), olivine (Fo_{60-85}) and leucite pseudomorphed by sanidine+nepheline set in a glassy groundmass having microlites of clinopyroxene±olivine, Ti-magnetite±ilmenite, Ti-phlogopite-biotite, alkali feldspar (Or_{15-88}), nepheline-analcime ($Ne_{44-59}Ks_{17-26}$). Phenocrystal plagioclase (up to An_{74}) is also present. Accessory phases are amphibole (pargasite-kaersutite) and apatite±zircon. Phonolites are characterized by phenocrysts of leucite-pseudomorphs, alkali feldspar (Or_{47-75}), clinopyroxene ($Wo_{48-50}Fs_{11-34}$), Fe-pargasite, nepheline±biotite±titanite±melanite (Ti-andradite up to 68

wt%)±magnetite or haematite. Glassy groundmass contains microlites of alkali feldspar, nepheline, clinopyroxene±Ti-andradite±magnetite. Haematite is found replacing magnetite or as a common groundmass constituent in peralkaline phonolites.

Table 1. Averages of representative chemical analyses (recalculated to 100 wt% on anhydrous basis; in parentheses, standard deviation) of tholeiites from ASV (Comin-Chiaramonti et al., 1993, 1996a, b). L-Ti and H-Ti tholeiites according to Bellieni et al. (1984, 1986a). The ε time-integrated notations are calculated using the present day bulk-Earth parameters (Faure, 2001), i.e. UR=0.7047 ($^{87}Rb/^{86}Sr$=0.0816) and CHUR=0.512638 ($^{147}Sm/^{144}Nd$=0.1967. Mg#: molar ratio MgO/(MgO+FeO).

Suite:	L-Ti	L-Ti	H-Ti	H-Ti
Tholeiite	Basalt	Andesibasalt	Basalt	Andesibasalt
N° of samples	(3)	(3)	(6)	(5)
Wt%				
SiO_2	50.20 (0.79)	53.06 (0.40)	50.83 (0.84)	50.52 (0.60)
TiO_2	1.40 (0.06)	1.36 (0.11)	2.58 (0.36)	3.19 (0.60)
Al_2O_3	14.64 (0.21)	13.78 (0.09)	13.98 (0.45)	14.25 (0.63)
FeOtot	12.73 (0.39)	13.42 (0.49)	13.54 (0.56)	14.55 (1.13)
MnO	0.19 (0.05)	0.25 (0.05)	0.21 (0.02)	0.21 (0.02)
MgO	7.36 (0.22)	5.53 (0.08)	5.13 (0.44)	4.19 (0.65)
CaO	10.63 (0.66)	8.55 (0.05)	9.65 (0.62)	8.56 (0.44)
Na_2O	2.36 (0.11)	2.66 (0.20)	2.61 (0.15)	2.49 (0.29)
K_2O	0.33 (0.05)	1.07 (0.18)	1.10 (0.17)	1.14 (0.10)
P_2O_5	0.15 (0.02)	0.19 (0.01)	0.37 (0.09)	0.36 (0.04)
Mg#	0.66	0.55	0.54	0.48
ppm				
La	6.2 (0.8)	9.0 (1.0)	25.3 (6.3)	26.0 (6.0)
Ce	16.0 (1.7)	21.0 (2.9)	60.4 (12.2)	50.0 (2.0)
Nd	11.1 (1.3)	14.1 (2.2)	28.3 (3.6)	25.0 (3.0)
Sm	3.4 (0.3)	4.3 (0.4)	7.7 (1.5)	6.8 (1.1)
Eu	1.2 (0.1)	1.5 (0.1)	2.2 (0.2)	1.9 (0.2)
Gd	4.3 (0.6)	5.4 (0.8)	7.7 (1.2)	6.9 (1.1)
Dy	4.8 (0.5)	6.0 (0.9)	6.3 (1.5)	5.7 (1.3)
Er	2.9 (0.4)	3.6 (0.6)	3.9 (1.3)	3.5 (0.9)
Yb	2.6 (0.4)	3.2 (0.4)	3.4 (1.2)	3.2 (1.0)
Lu	0.34 (0.07)	0.42 (0.09)	0.49 (0.15)	0.50 (0.19)
Cr	325 (27)	62 (1)	119 (15)	48 (2)
Ni	103 (18)	55 (7)	60 (15)	54 (12)
Rb	13 (4)	13 (1)	24 (3)	33 (11)
Sr	188 (42)	187 (2)	386 (90)	334 (15)
Ba	154 (19)	190 (4)	409 (78)	347 (37)
Th	1.1 (0.1).	1.7 (0.2)	2.0 (0.1)	3.0 (0.2)
U	0.24 (0.05)	0.37 (0.08)	0.43 (0.08)	0.65 (0.04)
Ta	0.28 (0..04)	0.42 (0.07)	1.2 (0.3)	1.8 (0.4)
Nb	4.0 (1.0)	6.1 (1.0)	13 (2)	20 (1)
Zr	83 (10)	113 (2)	190 (36)	197 (6)
Y	28 (2)	42 (1)	33 (4)	36 (3)
measured				
$(^{87}Sr/^{86}Sr)$	0.70548 (20)	0.70535 (20)	0.70617 (21)	0.70620 (18)
$(^{143}Nd/^{144}Nd)$	0.51271 (9)	0.51272 (10)	0.51239 (2)	0.51240 (1)
Age 131.6				
Initial ratio				
$(^{87}Sr/^{86}Sr)i$	0.70502	0.70456	0.70576	0.70554
$(^{143}Nd/^{144}Nd)i$	0.51256	0.51256	0.51225	0.51226
T_{DM}	1991	1976	2127	2037
R1	2037	1929	1758	1722
R2	1789	1459	1561	1403
εSr	6.70	0.12	17.16	14.12
εNd	1.60	1.79	-4.30	-4.10

The intrusive equivalents (theralites, essexitic gabbros, ijolites and essexites) are holocrystalline, seriate, with diopsidic pyroxene ($Wo_{44-51}Fs_{8-17}$), olivine (Fo_{75-82} to Fo_{44-66}), mica

(Ti-phlogopite to Ti-biotite), Ti-magnetite, alkali feldspar, nepheline ($Ne_{64-80}Ks_{20-36}$)±leucite±amphibole. "Intrusive" leucite and leucite pseudomorphed by analcime and plagioclase are common, testifying to subvolcanic conditions (Comin-Chiaramonti and Gomes, 1996). Cumulitic textures are represented by clinopyroxene with alkali feldspar+nepheline+carbonate as intercumulus phases.

On the wole, the temperatures calculated for the mineral assemblages span from 1250 to 1200°C and from 1130 to 1080°C, pheno and microphenocrysts, respectively, under about 1kb H_2O pressure, and around 1000°C under atmospheric pressure; lower temperatures, e.g. 900-700°C, suggest possible subsolidus exchange reactions (e.g., albitization). Magnetite-ilmenite pairs define temperatures between 1000 and 1100°C, along the NNO buffer (Comin-Chiaramonti et al., 1999).

Notably, the B-P suite is also characterized by carbonatitic magmatism, although it is very limited in volume: a silico-beforsitic flow is present in the Sapucai lava sequences, and as "ocelli" at the Canãda and Cerro E Santa Helena K-alkaline complexes (Comin-Chiaramonti et al., 1992b). These primary carbonates are relevant as they reveal a CO_2 imprinting after the tholeiitic magmatism.

AB-T suite. Alkali gabbros, syenogabbros and syenodiorites are usually porphyritic and seriate in texture. They contain clinopyroxene ($Wo_{43-50}Fs_{6-14}$), olivine (Fo_{43-82}), Ti-biotite, Ti-magnetite±ilmenite, plagioclase (An_{31-78}), alkali feldspar (Or_{60-84}) and interstitial nepheline-analcime ($Ne_{37-82}Ks_{15-23}$) and alkali feldspar (Or_{80-97}). Accessories are apatite±amphibole±titanite±zircon. Nepheline syenites and syenites are texturally equi- to subequigranular and seriate. The rock types are characterized by alkali feldspar (Or_{32-63}), clinopyroxene ($Wo_{43-48}Fs_{10-32}$), nepheline (Ne_{85}) and hastingsite. Common accessories include titanite and apatite±carbonate±zircon.

Alkali basalts, trachybasalts and trachyandesites are porphyritic rocks exhibiting phenocrysts and/or microphenocrysts of clinopyroxene ($Wo_{44-49}Fs_{7-15}$), olivine (Fo_{65-83}), plagioclase (An_{28-76}), magnetite, biotite set in a glassy groundmasses consisting of microlites of clinopyroxene ($Wo_{46-49}Fs_{13-18}$), magnetite, ilmenite, biotite, plagioclase (An_{20-45}), alkali feldspar (Or_{52-65}), nepheline-analcime ($Ne_{37-73}Ks_{22-38}$), amphibole, and apatite±titanite±zircon.

Trachyphonolites and trachytes are porphyritic to aphyric. The phenocrysts are alkali feldspar (Or_{60-65})±clinopyroxene ($Wo_{46-49}Fs_{14-20}$)±plagioclase (An_{14-16}), pseudomorphosed leucite, amphibole and biotite in a hypocrystalline to glassy groundmass containing microlites of alkali feldspar, biotite, and clinopyroxene±biotite±amphibole±magnetite±Ti-andradite±haematite.

Notably, the equilibration temperatures of the mineral assemblages are very similar to those suggested for the B-P suite (Comin-Chiaramonti et al., 1990, 1992a, 1997).

The differentiation history of the potassic ASV magmas remained largely into the stability fields of the ferromagnesian phases (Comin-Chiaramonti et al., 1999), i.e. olivine+clinopyroxene, in the system Mg_2SiO_4-$KAlSiO_4$ (Comin-Chiaramonti et al., 1992a, 1997; cf. Edgar, 1980), suggesting that relatively high temperature subvolcanic conditions were prevalent. Moreover, the extreme differentiates from both B-P and AB-T suites approaches to the composition of peralkaline residua, pointing to an extensive subvolcanic crystallization of K-rich, aluminous phases likely phlogopite and leucite, at least for the B-P suite (Cundari and Ferguson, 1982).

4.3. The sodic rocks

They consist mainly of ankaratrites+(mela)nephelinites (45%) and phonolites (42%) according to Comin-Chiaramonti et al. (1993, 1996b, 1997). Representative chemical analyses are reported in Table 4.

Phenocrysts-microphenocrysts in ankaratrites and nephelinites (Comin-Chiaramonti et al., 2009, and therein references) are characterized by olivine (phenocrysts 1-7 vol%, Fo_{89-85} mole%; 1-6 vol% microphenocrysts, Fo_{82-77} mole%), clinopyroxene (phenocrysts 1-6 vol%, mg# ~0.8) and titanomagnetite (0.3-0.7 vol%, up to 38 ulv. mole%), and occasionally phlogopite

microphenocrysts. The hypocrystalline groundmass contains clinopyroxene (39-46% vol%, mg# ~0.75), olivine (3-6 vol%, Fo_{74-76} mole%), titanomagnetite (4-7 vol%, up to 43% ulv. mole%), nepheline (16-21 vol%), and glass (11-25 vol%).

Table 2. Representative chemical analyses (recalculated to 100 wt% on anhydrous basis; in parentheses, standard deviation) of K-alkaline rocks (B-P suite, effusive and intrusive equivalents and dykes) from ASV (Comin-Chiaramonti and Gomes, 1996; Comin-Chiaramonti et al., 1992a, 1997). Analysis of a silico-beforsitic flow, on anhydrous basis, is also shown (Comin-Chiaramonti et al. 1992b; Castorina et al., 1997). Ages as in Comin-Chiaramonti et al. (2007a).

Suite B-P

K-alkaline	Basanite	Tephrite	Phonotephrite	Phonolite	Silico-beforsite 22%dolomite	Silico-beforsite Carb. fraction
N° of samples	(4)	(6)	(4)	(1)	(1)	
Wt%						
SiO_2	46.95 (2.14)	49.08 (1.31)	52.36 (1.64)	48.69	49.05	-
TiO_2	1.78 (0.19)	1.94 (0.26)	1.42 (0.19)	1.97	1.94	-
Al_2O_3	12.84 (1.63)	12.94 (1.17)	17.27 (1.24)	16.42	15.32	-
FeOtot	10.20 (1.80)	10.02 (0.97)	7.39 (0.75)	8.45	9.60	-
MnO	0.18 (0.03)	0.17 (0.02)	0.15 (0.02)	0.15	0.17	-
MgO	9.95 (2.02)	7.88 (1.64)	3.66 (0.58)	3.86	5.28	-
CaO	11.31 (1.41)	9.36 (0.85)	7.00 (1.02)	6.96	8.81	-
Na_2O	2.42 (0.61)	2.99 (0.92)	4.34 (0.58)	3.79	3.50	-
K_2O	3.78 (1.18)	4.99 (1.24)	5.73 (0.17)	8.60	6.14	-
P_2O_5	0.59 (0.21)	0.66 (0.18)	0.58 (0.07)	0.69	0.34	-
						-
Mg#	0.67	0.62	0.51	0.45	-	-
ppm						
La	82.1 (19.0)	91.2 (13.0)	93.3 (13.6)	98	80	239.06
Ce	162.6 (30.4)	164.1 (18.1)	170.0 (25.0)	186	145	420.34
Nd	64.4 (10.9)	69.3 (4.9)	66.6 (12.1)	73.2	62	159.89
Sm	12.8 (2.4)	12.8 (3.6)	11.4 (1.6)	15.1	11.3	19.06
Eu	3.0 (0.6)	3.0 (0.4)	2.8 (0.3)	2.02	2.3	3.90
Gd	7.4 (1.9)	6.8 (1.1)	7.1 (0.6)	5.93	8.8	14.90
Dy	4.4 (0.6)	3.6 (0.2)	3.9 (0.4)	2.86	6.2	10.57
Er	1.9 (0.4)	1.7 (0.3)	1.9 (0.3)	1.59	3.3	5.40
Yb	1.6 (0.1)	1.4 (0.4)	1.5 (0.3)	1.59	1.9	3.16
Lu	0.25 (0.01)	0.21 (0.06)	0.26 (0.06)	0.23	0.28	0.32
Cr	275 (106)	378 (260)	36 (23)	53	51	-
Ni	81 (29)	111 (42)	28 (18)	22	18	-
Rb	88 (18)	117 (51)	111 (35)	260	148	0.21
Sr	1134 (279)	1661 (227)	1569 (10)	1626	1126	268
Ba	1179(252)	1582 (147)	1462 (215)	1935	1350	-
Th	14.4 (9.9).	11.4 (3.5)	12.1 (1.6)	12.7	15.2	-
U	2.9 (1.0)	2.4 (0.7)	2.5 (0.1)	3.5	4.2	-
Ta	3.2 (0..2)	3.0 (0.7)	3.2 (0.3)	5.1	2.7	-
Nb	38.0 (7.0)	44 (10)	47 (1)	62	35	-
Zr	246 (42)	282 (91)	259 (35)	365	280	-
Y	14.0 (2.8)	17.3 (6.7)	18.9 (3.0)	13	18	23.75
measured						
$(^{87}Sr/^{86}Sr)$	0.70761 (4)	0.70774 (3)	0.70727 (4)	0.70752 (2)	0.70807 (2)	0.70762 (3)
$(^{143}Nd/^{144}Nd)$	0.51182(4)	0.51171 (1)	0.51160 (4)	0.51187 (2)	0.511804 (6)	0.511371 (8)
Age	130	129	124	125	128	-
Initial ratio						
$(^{87}Sr/^{86}Sr)i$	0.70697	0.70716	0.70671	0.70645	0.70700	0.70717
$(^{143}Nd/^{144}Nd)i$	0.51172	0.51162	0.51152	0.51177	0.51171	0.51131
T_{DM}	2049	2042	2043	2067	1884	1844
R1	1054	713	365	-397	-	-
R2	1955	1646	1269	1258	-	-
εSr	34.31	37.04	30.58	26.88	34.7	34.17
εNd	-14.69	-16.71	-18.78	-13.83	-14.8	-22.7

Table 3. Representative chemical analyses (recalculated to 100 wt% on anhydrous basis; in parentheses, standard deviation) of K-alkaline rocks (AB-T suite, effusive and intrusive equivalents and dykes) from ASV (Comin-Chiaramonti et al. 1992a; Castorina et al., 1997). Ages as in Comin-Chiaramonti et al. (2007a).

Suite AB-T K-alkaline	Alkaline basalt	Trachybasalt	Trachyandesite	Trachyphonolite	Trachyte
N° of samples	(3)	(3)	(7)	(5)	(1)
Wt%					
SiO_2	48.69 (1.50)	50.90 (1.56)	53.16 (1.18)	58.25 (1.44)	58.95
TiO_2	1.69 (0.48)	1.49 (0.31)	1.42 (0.21)	0.91 (0.23)	1.94
Al_2O_3	15.17 (1.86)	17.07 (1.06)	16.99 (1.45)	18.39 (1.01)	19.03
FeOtot	10.31 (0.76)	9.04 (0.57)	7.96 (0.75)	4.87 (1.51)	4.49
MnO	0.19 (0.01)	0.16 (0.02)	0.15 (0.02)	0.16 (0.01)	0.12
MgO	6.71 (0.89)	5.01 (0.24)	4.03 (0.58)	0.89 (0.90)	1.69
CaO	11.09 (0.63)	8.58 (1.11)	6.95 (0.66)	4.59 (1.09)	3.37
Na_2O	3.16 (0.42)	3.64 (0.44)	4.10 (0.38)	5.89 (1.38)	4.21
K_2O	2.46 (0.42)	3.65 (0.72)	4.61 (1.06)	5.76 (1.13)	7.00
P_2O_5	0.55 (0.36)	0.50 (0.17)	0.55 (0.09)	0.29 (0.10)	0.25
Mg#	0.58	0.53	0.51	0.32	0.40
ppm					
La	51.2 (16.0)	54.0 (18.6)	82.8 (29.7)	154.0 (33.9)	136
Ce	106.7 (24.4)	109.0 (21.0)	154.2 (55.7)	261.1 (44.2))	206
Nd	52.7 (19.7)	47.9 (12.9)	64.7 (15.7)	84.0 (17.7)	78
Sm	10.5 (1.6)	9.4 (30.5)	10.8 (2.1)	12.7 (3.5)	15.1
Eu	2.8 (1.0)	2.5 (0.3)	2.8 (0.5)	3.28 (0.8)	3.9
Gd	6.8 (2.4)	6.0 (1.2)	6.4 (1.0)	5.70 (1.6)	9.4
Dy	4.1 (0.7)	4.2 (0.6)	4.2 (0.7)	5,44 (1.1)	6.3
Er	1.7 (0.1)	1.8 (0.3)	1,6 (0.4)	2.59 (0.58)	2.3
Yb	1.5 (0.1)	1.6 (0.4)	1.6 (0.4)	2.25 (0.46)	2.0
Lu	0.22 (0.05)	0.24 (0.03)	0.28 (0.08)	0.35 (0.08)	0.31
Cr	143 (24)	92 (59)	38 (34)	10 (6)	8
Ni	49 (6)	31 (18)	17 (12)	6 (2)	2
Rb	53 (13)	98 (16)	87 (20)	7 (3)	133
Sr	1573 (263)	1389 (407)	1474 (194)	77 (34)	600
Ba	1033(321)	1280 (170)	1211 (168)	1377 (215)	1726
Th	4.3 (2.1).	7.9 (1.5)	14.6 (8.5)	31.7 (8.5)	-
U	1.3 (0.5)	1.7 (0.6)	3.4 (3.0)	9.5 (3.3)	-
Ta	2.3 (1.1)	1.6 (0.4)	2.8 (0.7)	2.6 (0.6)	2.5
Nb	18.1 (9.0)	25.0 (6.0)	40 (12)	62 (18)	61
Zr	260 (31)	220 (33)	268 (14)	411 (128)	392
Y	14.5 (9.2)	14.6 (6.5)	19.5 (3.2)	25 (4)	23
measured					
$(^{87}Sr/^{86}Sr)$	0.70717 (4)	0.70721 (5)	0.70753 (4)	0.70752 (2)	0.70807 (2)
$(^{143}Nd/^{144}Nd)$	0.51185(4)	0.51170 (3)	0.51160 (4)	0.51187 (2)	0.51181 (6)
Age	125	119	129	125	128
Initial ratio					
$(^{87}Sr/^{86}Sr)i$	0.70693	0.70673	0.70709	0.70708	0.70639
$(^{143}Nd/^{144}Nd)i$	0.51175	0.51161	0.51151	0.51179	0.51171
T_{DM}	2009	2199	1999	1530	2001
R1	1215	954	749	545	649
R2	1817	1501	1277	1014	818
εSr	33.68	30.74	36.09	35.85	26.0
εNd	-14.16	-17.12	-18.68	-13.31	-14.9

Table 4. Representative chemical analyses (recalculated to 100 wt% on anhydrous basis; in parentheses, standard deviation) of Na-alkaline rocks from ASV (Comin-Chiaramonti et al. 1992a; Castorina et al., 1997). Ages as in Comin-Chiaramonti et al. (2007a).

Suite: Sodic Na-Alkaline	Ankaratrite	Ankaratrite	Ankaratrite	Melanephelinite	Peralkaline Phonolite
N° of samples	(1)	(1)	(5)	(1)	(1)
Wt%					
SiO_2	43.71	43.97	43.29 (0.65)	45.67	55.96
TiO_2	2.39	2.12	2.50 (0.48)	2.21	0.43
Al_2O_3	14.84	13.87	13.42(0.95)	14.83	21,19
FeOtot	10.01	10.44	10.71 (0.40)	7.83	4.04
MnO	0.18	0.21	0.19 (0.01)	0.20	0.22
MgO	10.07	9.87	11.47 (1.23)	8.92	0.21
CaO	12.06	10.81	11.82 (0.28)	10.78	1.34
Na_2O	5.15	6.00	4.12 (0.21)	6.73	10.77
K_2O	0.89	1.51	1.61 (0.32)	1.54	5.76
P_2O_5	0.90	1.22	0.88 (0.14)	1.28	0.08
Mg#	0.74	0.72	0.69	0.58	0.22
p.p.m.					
La	81	119	84.2 (12.4)	118	120
Ce	145	186	162.8 (24.3)	190	191
Nd	43.4	63.7	55.2 (8.5)	65.1	65
Sm	8.15	11.23	9.4 (1.2)	11.45	11
Eu	1.89	2.15	2.7 (0.3)	2.18	-
Gd	5.77	5.16	6.7 (0.7)	5.23	-
Dy	4.81	4.81	5.5 (0.7)	5.00	-
Er	2.13	2.75	2.4 (0.3)	2.86	-
Yb	1.65	1.79	1.8 (0.3)	1.87	-
Lu	0.23	0.27	0.27 (0.04)	0.28	-
Cr	542	648	490 (74)	470	2
Ni	207	273	249 (48)	239	6
Rb	22	59	53 (13)	63	60
Sr	1016	1013	1109 (63)	1095	654
Ba	1090	980	1090(95)	1094	367
Th	10.5	10.5	11.0 (2.4).	11.6	--
U	2.3	2.3	2.4 (0.5)	2.5	--
Ta	5.9	5.9	8.4 (1.0)	6.5	-
Nb	86	101	105 (13)	113	-
Zr	152	234	250 (43)	228	955
Y	26	33	29 (4)	32	39
measured					
$(^{87}Sr/^{86}Sr)$	0.70395 (1)	0.70374 (1)	0.70381 (8)	0.70392 (1)	0.70405 (2)
$(^{143}Nd/^{144}Nd)$	0.51275 (1)	0.51276 (1)	0.512724(61)	0.51274 (2)	0.51268 (2)
Age:	46	46	46	50	60
Initial ratio					
$(^{87}Sr/^{86}Sr)i$	0.70391	0.70364	0.70373	0.70381	0.70384
$(^{143}Nd/^{144}Nd)i$	0.51272	0.51273	0.51269	0.51271	0.51264
TDM	581	532	562	558	617
R1	582	100	682	18	-1567
R2	2080	1918	2096	1886	570
εSr	-10.42	-14.30	-13.05	-11.79	-11.19
εNd	2.67	2.91	2.23	2.57	1.54

Phonolites are typically microphyric to hypocrystalline with alkali feldspar phenocrysts or microphenocrysts ($Or_{43–83}$), nepheline ($Ne_{67–79}$), occasionally altered to cancrinite, acmitic clinopyroxene (acmite up to 63 wt%) and ferroedenite-ferropargasite amphibole. Haüyne, mica, haematite and zircon are typical accessory minerals. Analcime occurs as a nepheline pseudomorph. Ti-andradite and titanite pheno-microphenocrysts are present in some dykes (Comin-Chiaramonti et al., 1997).

Melting models indicate that these rocks derived from liquids representing about 4-6% degrees of a garnet peridotite source and crystallization temperatures are between 1200-1000°C (Comin-

Chiaramonti et al., 1991, 1997). Notably, lherzolite, harzburgite and dunite mantle xenoliths and xenocrystic debris are common and abundant in the ankaratrites and nephelinites (Demarchi et al., 1988) from eastern ASV (Fig. 3).

4.4. Mantle Xenoliths

The xenoliths are mainly spinel-lherzolites, harzburgites and subordinate dunites. The dominant texture is protogranular, rarely tabular or porphyroclastic (Demarchi et al., 1988). The Paraguay mantle xenoliths contain variable amounts of glassy patches (blebs), and glassy drops in clinopyroxenes (Comin-Chiaramonti et al., 2001). The latters show an overprinted spongy texture (Demarchi et al., 1988). The blebs (whole composition: mg# 0.88-0.91) consist mainly of a glassy matrix having microlites of olivine (mg# 0.91-0.92), clinopyroxene (mg# 0.91-0.93), Cr-spinel and (rarely) phlogopite (mg# 0.86-0.92).

According to Comin-Chiaramonti et al. (2001) and Wang et al. (2007), they were formed by decompression melting of amphibole and phlogopite.

The Paraguayan xenoliths are characterized by a large range of K_2O contents (0.02 to 0.51 wt%). Some xenoliths have K_2O abundances comparable or even higher than those reported for metasomatized mantle peridotites (cf. Roden et al., 1984), resembling in some case to amphibole-mica-apatite bearing mantle-xenolith suites (cf. O'Reilly and Griffin, 1988). K_2O contents and the abundance of blebs and glassy drops allow to group the Paraguay xenoliths into two main suites, i.e. a low-K suite (LK, K_2O <0.15 wt%), and a high-K suite, the latter with abundant glassy drops and/or variable amounts of blebs and spongy clinopyroxenes (HK, K_2O ≥0.2 wt%). Representative analyses are listed in Table 5 and complete sets of chemical analyses are in Demarchi et al. (1988).

Based on the Spera's (1984) approach, Comin-Chiaramonti et al. (1991) suggested that the transportation of the xenoliths to the surface took place in a very short time, e.g. less than nine days (assuming a diameter of 45 cm, corresponding to the largest xenolith size, a density of 3.3 g/cm^3 and an origin of the hosting liquids from depth ~70-75 km, i.e. ~boundary between garnet and spinel peridotite).

Coherent variations of major element contents in both suites follow a dunite-lherzolite sequence trending to the mantle composition (Demarchi et al., 1988). The population is represented mainly by lherzolitic-harzburgitic (dunitic) compositions, mostly with a 0.55-0.63 range of $(SiO_2+Al_2O_3)/(MgO+FeO_t)$ molar ratio. The residual character of the harzburgitic mantle xenoliths (believed to be consistent with melting and basalt-component removal) is also indicated by the decrease in the cpx/opx modal ratio with decreasing modal cpx, which fits the model variation trend induced by partial melting of lherzolite (Comin-Chiaramonti et al., 2001, cf. Rivalenti et al., 1996).

These mantle xenoliths provide an opportunity for a direct sampling of the subcontinental mantle in ASV. Studies on mantle xenoliths have pointed out that incompatible trace elements, radiogenic isotopes and major element chemistry are largely decoupled from the coherent variation that would be expected by progressive melt extraction from a peridotite at mantle conditions (Frey and Green, 1979). In particular, variable enrichments of incompatible elements are commonly observed in contradiction to the refractory composition of the majority of the xenoliths, thus requiring additional processes besides partial melting and fractionation.

Such processes have been generally called *metasomatic* by Frey and Hawkesworth (1987). Metasomatism of residual peridotites by volatile-charged fluids or small-volume melts carrying incompatible elements causes different types of enrichment. Metasomatically changed parent/daughter element ratios could develop isotopic inhomogeneities by radioactive in situ decay in a non-convective, lithospheric mantle. Thus, geochemical and isotopic data of mantle xenoliths provide valuable information about the nature and timing of differentiation, and possible metasomatism of mantle domains.

Equilibration temperatures for orthopyroxene-clinopyroxene pairs (Wells, 1977) and for olivine-spinel pairs (Fabriès, 1979) range between 862 and 1075°C and between 748 and 968°C, respectively. Intracrystalline temperatures (Mercier, 1980; Mercier et al., 1984; Sen et al., 1993) for

clinopyroxene and orthopyroxene pairs vary as average between 936 and 1033°C for the LK suite, and between 920 and 1120°C for the HK suite. The pressures are roughly in the range of 1.1-2.3 GPa for both suites, with the higher values related to the more depleted xenoliths of the LK suite (Comin-Chiaramonti et al., 2001, 2009).

Table 5. Average chemical analyses (recalculated to 100 wt% on anhydrous basis; in parentheses, standard deviation) of mantle xenoliths (LK and HK suites, $K_2O<0.15$ wt% and >0.2 wt%, respectively) from ASV (Demarchi et al., 1988; Comin-Chiaramonti et al., 2001, 2009 and unpublished data). The age is the average of ages of Table 4. The bleb is a representative glassy drop in a H-K harzburgite (Demarchi, 1989; Comin-Chiaramonti, 2001).

Whole-rock	L-K Lherzolite	L-K Harzburgite	H-K Lherzolite	H-K Harzburgite	H-K Bleb
N° of samples	(5)	(6)	(3)	(2)	(1)
Wt%					
SiO_2	44.02 (1.15)	43.95 (0.35)	44.65 (0.11)	44.63 (0.20)	46.15
TiO_2	0.03 (0.02)	0.01 (0.00)	0.07 (0.03)	0.02 (0.00)	0.70
Al_2O_3	1.76 (0.86)	1.14 (0.50)	2.37 (0.04)	1.36 (0.03)	10.10
FeOtot	7.97 (0.13)	7.85 (0.22)	7.92 (0.24)	7.52 (0.01)	6.74
MnO	0.12 (0.01)	0.11 (0.00)	0.11 (0.01)	0.11 (0.00)	0.14
MgO	44.17 (1.87)	45.58 (1.60)	41.55 (0.46)	44.76 (0.21)	23.67
CaO	1.75 (0.86)	1.18 80.69)	2.64 (0.23)	1.12 (0.02)	6.56
Na_2O	0.12 (0.01)	0.10 (0.05)	0.28 (0.01)	0.16 (0.01)	2.00
K_2O	0.09 (0.04)	0.06 (0.04)	0.39 (0.10)	0.32 (0.00)	3.10
P_2O_5	0.21 (0.10)	0.01 (0.01)	0.01 (0.00)	0.02 (0.00)	0.83
ppm					
La	1.69 (0.12)	2.87 (0.51)	2.66 (0.52)	6.71 (0.69)	77.39
Ce	1.53 (0.09)	4.09 (0.75)	3.35 (0.67)	8.45 (0.81)	106.25
Nd	0.20 (0.01)	0.28 (0.16)	0.96 (0.55)	2.42 (0.25)	27.74
Sm	0.012 (0.004)	0.038 (0.015)	0.260 (0.014)	0.51 (0.20)	4.16
Eu	0.001 (0.001)	0.006 (0.002)	0.010 (0.01)	0.020 (0.006)	1.00
Gd	0.07 (0.008)	0.04 (0.01)	0.37 (0.02)	0.74 (0.03)	2.92
Dy	0.10 (0.01)	0.05 (0.01)	0.43 (0.02)	0.91 (0.04)	2.61
Er	0.07 (0.001)	0.05 (0.01)	0.30 (0.01)	0.65 (0.06)	1.68
Yb	0.07 (0.001)	0.08 (0.01)	0.29 (0.01)	0.63 (0.03)	1.23
Lu	-	-	-	-	
Cr	2601 (350)	2421 (357)	2360 (88)	2635 (30)	38114
Ni	2307 (160)	2309 (102)	2120 (4)	2307 (73)	1124
Rb	3.33 (9.51)	2.67 (1.63)	7.50 (2.12)	6.00 (1.41)	120
Sr	22.41 (10.47)	11.15 (4.58)	28.89 (10.29)	64.67 (7.62)	1414
Ba	20.0 (10.0)	4.67 (1.18)	40 (8)	34.5 (14.8)	1781
Th	-	-	-	-	-
U	-	-	-	-	-
Ta	-		-	-	-
Nb	5.91 (0.58)	1.78 (0.20)	6.39 (1.77)	6.98 (1.01)	155
Zr	5.95 (0.41)	6.08 (0.45)	6.90 (0.13)	7.86 (0.93)	189
Y	0.51 (0.10)	0.72 (0.09)	2.62 (0.09)	5.70 (1.08)	14.70
measured					
$(^{87}Sr/^{86}Sr)$	0.70426 (0.00005)	0.70421 (0.00038)	0.70416 (0.00006)	0.70395 (0.00002)	-
$(^{143}Nd/^{144}Nd)$	0.51264 (0.00007)	0.51275 (0.00039)	0.51299 (0.00033)	0.51288 (0.00005)	-
Age	(50±6)	(50±6)	(50±6)	(50±6)	-
Initial ratio	0.70398	0.70376	0.70367	0.70377	-
$(^{87}Sr/^{86}Sr)i$	0.51263	0.51272	0.51294	0.51285	-
$(^{143}Nd/^{144}Nd)i$					
T_{DM}	427	448	446	453	-
εSr	-9.40	-12.55	-13.80	-12.31	-
εNd	1.06	2.92	7.08	5.16	-

The oxygen isotope compositions on separates of clinopyroxene and coexisting olivine ($\delta^{18}O$‰) vary from 5.5 to 6.0‰, and from 5.0 to 6.1‰, respectively (Comin-Chiaramonti et al., 2009). These

measured isotopic ratios are in the range of values for worldwide mantle phases: olivine, 4.4 to 7.5‰, and clinopyroxene, 4.8 to 6.7‰ (Chiba et al., 1989; Mattey et al., 1994); and for South America mantle xenoliths: olivine, 4.9 to 6.4‰, and clinopyroxene, 5.0 to 6.0‰ (Kyser, 1990). The calculated Cpx-Ol isotopic temperatures (Kyser et al., 1981) are around 970-1070°C and 1030-1130°C (LK) and 1100-1180°C (HK), suggesting equilibration temperatures higher in the HK suite than in LK suite.

It can be observed that the highest temperature of the HK suite is substantially due to higher $\delta^{18}O\%$ in olivine than $\delta^{18}O\%$ in clinopyroxene: according to [73] the relatively low $\delta^{18}O$ in the pyroxenes reflects metasomatism by a silicate melt from subducted altered oceanic crust. So the Paraguayan HK suite should be the best candidate to a subduction-linked environment.

The investigated ASV clinopyroxenes [74] have V(Cell) and V(M1) sites intermediate between those of plagioclase- and garnet-bearing mantle peridotites, i.e., in a pressure range between 1.2 and 2.2 GPa. Thus, also the isotopic and crystallographic results fit the same inter and intracrystalline data.

On the whole, the ASV xenoliths define a geotherm (Comin-Chiaramonti et al., 2009) that, starting at about 830°C and 1.0 GPa, at the transition mantle-crust, intersects the hydrous peridotite solidus at about 1140°C and 2.1-2.2 GPa in the spinel peridotite facies, near to the transition with the garnet peridotite facies, believed to be the source of the sodic alkaline magmatism.

5. Geochemistry

Incompatible Elements (IE), Large Ion Lithophile Element (LILE), and High Field Strength Element (HFSE) ratios, coupled with the Sr-Nd isotopic compositions, appear to indicate that the magmatic events present in ASV were generated from geochemically distinct (enriched vs. depleted) mantle sources (Antonini et al., 2005, and therein references).

5.1. Incompatible elements

The IE patterns (mantle normalized) for the various and different magmatic rock-groups are diagrammatically represented in Fig. 6.

The L-Ti and H-Ti ASV tholeiites are distinct in terms of their relatively low elemental abundances and high LILE/HFSE ratios. In particular, their marked Ta-Nb negative spikes are similar to those of the potassic alkaline magmas from ASV, but clearly different in comparison to the Cenozoic sodic alkaline rocks from the same area.

The suites are similarly enriched in REE and exhibit steep, subparallel LREE trends [$(La/Lu)_{CN}$=26-161, 17-62 and 11-46 for B-P, AB-T and Na rocks, respectively], which tend to flatten out for HREE [$(Dy/Lu)_{CN}$=1.24-1.96, 1.09-2.00 and 0.56-2.05 for B-P, AB-T and Na rocks, respectively], HK-dykes excepted. REE profiles with LREE enrichment and flat HREE suggest mantle sources which have been previously depleted by melt extraction and subsequently enriched (McKenzie and O'Nions, 1995).

Multi-elemental diagrams, normalized to a primordial mantle composition (Fig. 6), show a substantial overlap of B-P and AB-T compositions, negative Nb, Ta, P, Ti and Y spikes, and positive U, K and Sr anomalies. In general, B-P compositions are higher in Rb, K, Zr, Hf, Ti, Y, LREE and MREE than AB-T compositions. On the contrary, the Na rocks yielded La/Nb and La/Ta ratios close to unity, respectively, and Nb/K and Ta/K ratios greater than 1.0, respectively. Notably, the variations of incompatible elements of the AB-T compositions mimic to some extent those of the ASV H-Ti (and L-Ti) tholeiitic basalts, which approach the lower (Rb to Nd) and higher (Sm to Lu) elemental concentrations of that suite (Fig. 6).

In summary, substantial overlap in bulk-rock chemistry exists between the investigated B-P and AB-T rocks, both characterized by variable K/Na ratio, although the K types being dominant. REE and other incompatible elements show similar concentration levels and variation trends in the two suites. The mantle normalized incompatible element patterns of both ASV suites show strong

affinities, including negative "Ta-Nb-Ti anomalies", with the Paraná tholeiites (Comin-Chiaramonti et al., 1997).

On the whole, the geochemical features suggest that the enrichment processes were related to small-volume melts in a lithospheric mantle (Castorina et al., 1997; Comin-Chiaramonti et al., 1997, 2007a).
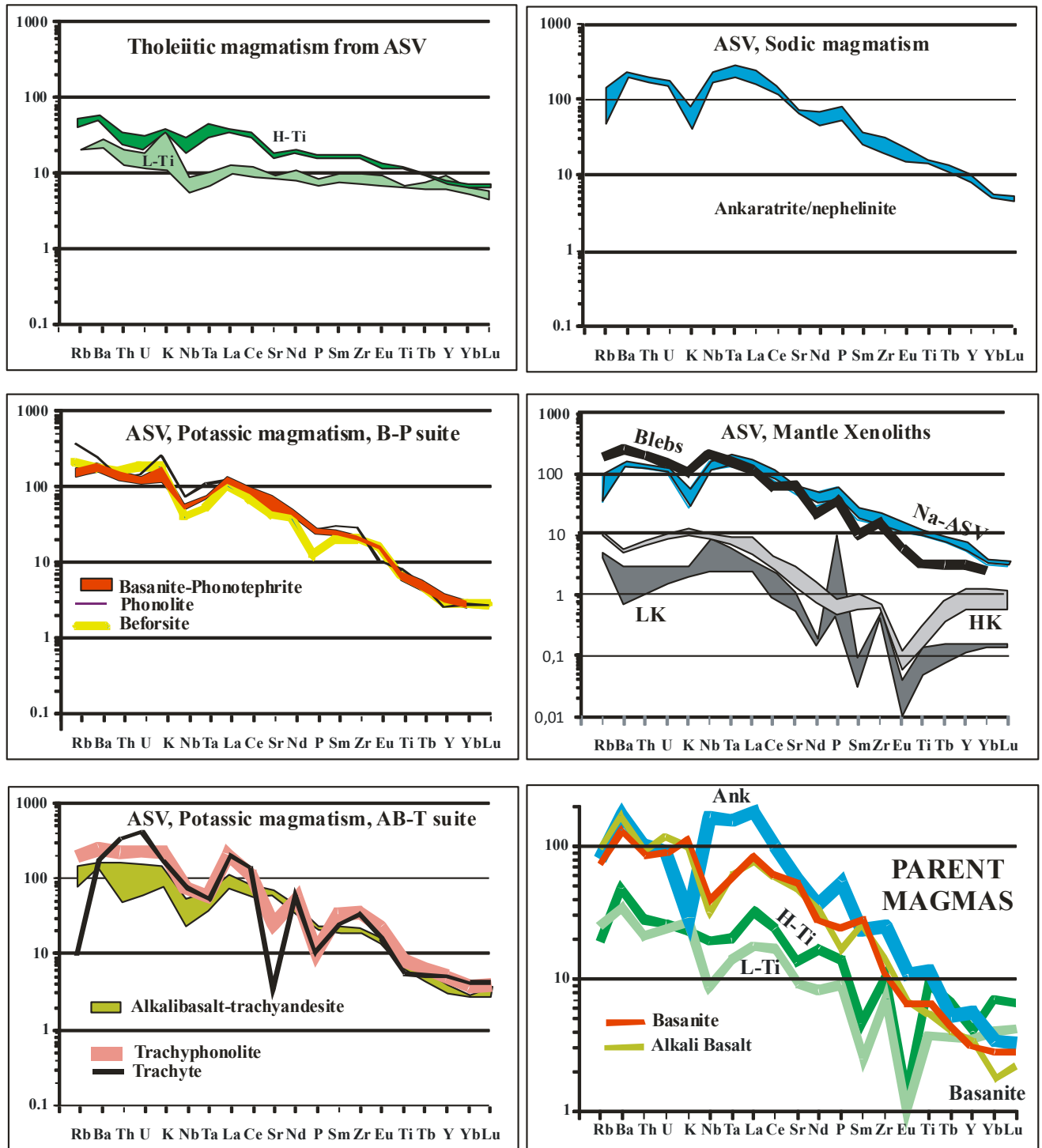
Fig. 6. ASV representative compositions (data source as in Tables 1 to 5): incompatible elements normalized to the primitive mantle (Sun and McDonough, 1989). **Parent magmas -** normalizations relative to the calculated parental magmas as proposed by Bellieni et al. (1986a, b), Piccirillo et al. (1988) and Comin-Chiaramonti (1997): L-Ti (mg# 0.64, Ni 250 ppm); H-Ti (mg# 0.60, Ni 250 ppm); basanite (mg# 0.74, Ni 710 ppm); alkaline basalt (mg# 0.74, Ni 323 ppm); ankaratrite (mg#0.70, Ni 993 ppm).

5.2 Mantle sources

The origin of the ASV magmas is closely related to, and probably constrained by, the geodynamic processes which promoted the generation of the adjacent and coeval magmatism in Brazil (Comin-Chiaramonti et al., 1997). The origin and emplacement of the ASV magmatism occurred before, during and after the opening of the South Atlantic and appears to be related to early stages of lithospheric extension, associated with an anomalously hot mantle (Piccirillo and Melfi, 1988; Hawkesworth et al., 1992; Turner et al., 1994). The K/Na and trace element variations and Sr-Nd isotope characteristics of the ASV suites support the view that the lithospheric mantle played an important role in their genesis as well as that of the Paraná flood basalts in Brazil (Piccirillo et al., 1989; Peate, 1992; Peate and Hawkesworth, 1996).

It should be noted that the most mafic tholeiitic and potassic ASV rock-types are relatively evolved compared with expected primary compositions (e.g. mg# >0.60-0.65, Ni >235 ppm), ankaratrite excepted. Possible ASV primary melts (e.g. mg# ~0.74) in equilibrium with Fo_{90-91} are expected to have fractionated olivine (Ol) and clinopyroxene (Cpx) at or near the mantle source and certainly during the ascent to the surface. Neglecting the effects of polythermal-polybaric fractionation on the chemistry of the fractionates, notional crystal fractions have been calculated to restore the selected ASV parental compositions to possible near-primary melts in equilibrium with their mantle sources (cf. Table 3 of Comin-Chiaramonti et al., 1997).

Mass balance calculations, starting from different garnet phlogopite peridotites (cf. Erlank et al., 1987; whole-rock and mineral compositions in Table 3 of Comin-Chiaramonti et al., 1997, and Table 10 of Bellieni et al., 1986b), indicate that the ASV primary melt compositions can be derived from high and relatively high melting degrees of anhydrous garnet or phlogopite-bearing peridotite, i.e. 12 and 30% for tholeiitic basalts (H-Ti and L-Ti, respectively) and 4-11% for the alkaline rock-types (Table 3 of Comin-Chiaramonti et al., 1997). However, the presence of a relative K enrichment in the ASV potassic and tholeiitic rocks (Fig. 6) suggests that a K-bearing phase (e.g. phlogopite) did not represent a residual phase during partial melting. Phlogopite, instead, was probably a residual phase in the mantle source(s) of the ASV sodic rocks. Notably, the parent melts (Fig. 6) show high abundances of IE and high LREE/HREE ratios, which require mantle sources enriched in IE before or subcontemporaneously with melting process (cf. Menzies and Wass, 1983): Nd model ages approximately indicate that the IE enrichment in the source mantle of the ASV tholeiitic and potassic rocks probably occurred during Paleoproterozoic times (mean 2.03±0.08 Ga), whereas those relative to the sodic rocks would be related to Late Neoproterozoic events (0.57±0.03 Ga). On the other hand, the mantle xenoliths display Nd model ages of 444±11 Ma (cf. Tables 1 to 5).

Concluding, the patterns of the mantle sources of the ASV potassic rocks (H-Ti and L-Ti tholeiites) are characterized by negative 'Ta-Nb-Ti' and positive Ba and Sm spikes. On the contrary, the patterns of the mantle sources of the ASV ankaratrites-melanephelinites show positive Ta-Nb and Zr, and negative K and Sm spikes. It seems, therefore, that the genesis of the ASV alkaline magmatism is dominated by a lithospheric mantle, characterized by small-scale heterogeneity, as also documented by the occurrence of bleb-like glass in spinel peridotite nodules from the ASV Na ultramafic rocks (Demarchi et al., 1988; Comin-Chiaramonti et al., 1991).

5.3. Sr-Nd isotopes

The investigated rocks from ASV show a large distribution on the Sr-Nd isotopic compositions (Fig. 7), describing a trend similar to the "low Nd" array of Hart and Zindler (1989; cf. also "Paraguay array" of Comin-Chiaramonti et al., 2007a). Due to the high Sr and Nd content of the most "primitive" alkaline rocks (and associated carbonatites) from Eastern Paraguay, Comin Chiaramonti et al. (1999) suggested that initial Sr-Nd isotopic ratios of such rock-types can be considered crustally uncontaminated and, as a result, representative of the isotopic composition of the mantle source(s).

The ASV potassic alkaline rocks have the highest initial (time integrated) Sr_i and the lowest initial Nd_i. Including the carbonatites of the BP-suite (Comin-Chiaramonti and Gomes, 1996, 2005), the Sr_i and Nd_i range from 0.70645 to 0.70716 and from 0.51151 to 0.51179, respectively (Tables 2 and 3). These values are quite distinct from those of the ASV Paleocene sodic rocks (ca. 60 Ma), which plots within the depleted quadrant (Sr_i=0.70364-0.70391, Nd_i=0.51264-0.51273, cf. Table 4), towards the HIMU-DMM depleted mantle components (Fig. 7). Notably, Sr_i and Nd_i of the tholeiites, believed by Comin-Chiaramonti et al. (1997) to be uncontaminated, both H- and L-Ti, are intermediate between the potassic and sodic rocks: 0.70456-0.70576 and 0.51225-0.51256, respectively (cf. Table 4): these values approach to the range of the Early Cretaceous uncontaminated tholeiites from the Paraná Basin (Piccirillo et al., 1989 and therein references), i.e. Sr_i=0.70527±0.00051 and Nd_i=0.51264±0.00011). To be stressed that the genesis of these tholeiites requires lithospheric mantle components, as represented by K-alkaline (and carbonatitic) rocks from the ASV (Comin-Chiaramonti 2007a, b).
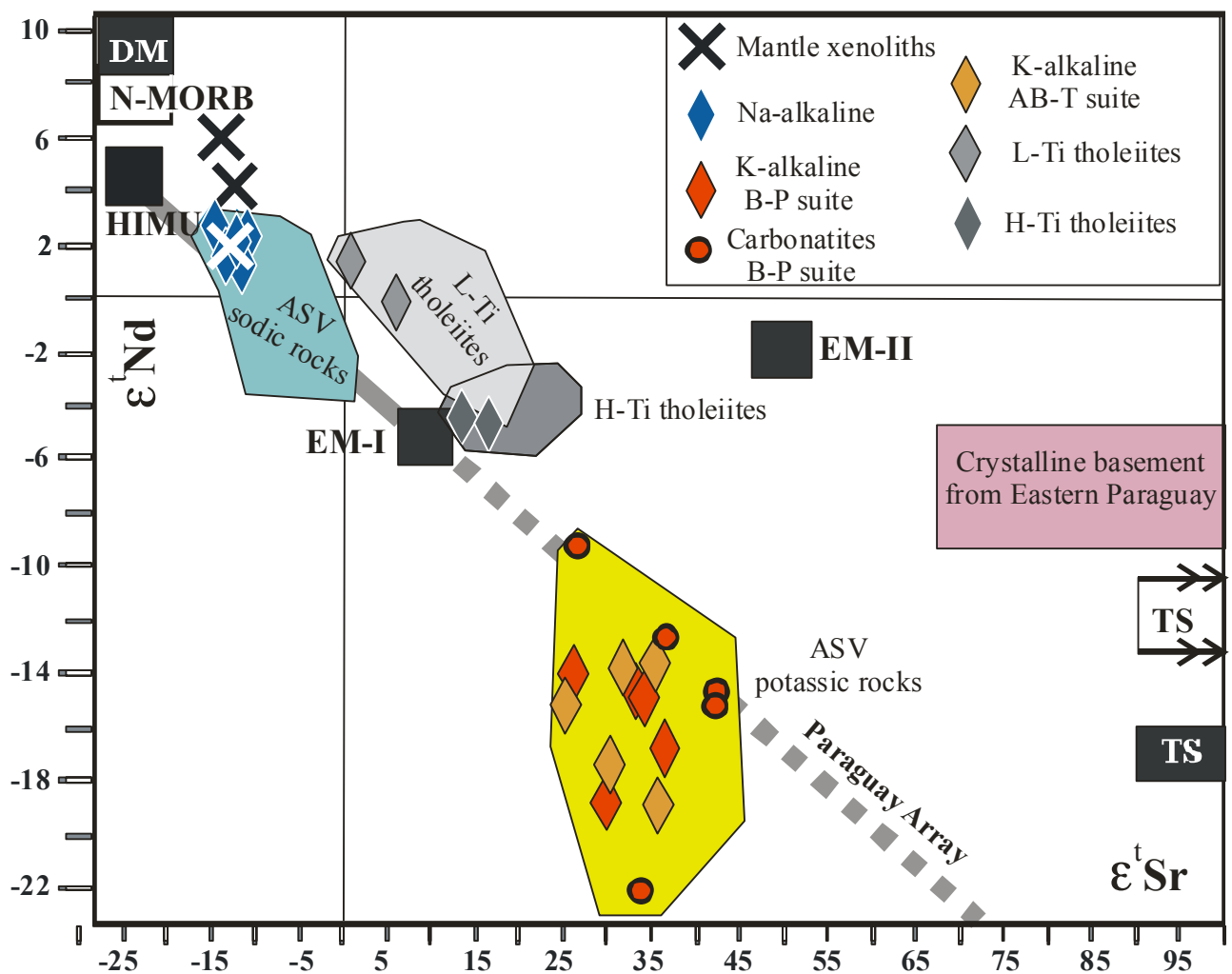
Fig. 7. Sr and Nd isotopic plot in ε−ε notation: $\varepsilon_t Sr$ vs. $\varepsilon_t Nd$ correlation diagram for igneous rocks from ASV. Data source: Tables 1 to 5 and Comin-Chiaramonti et al. (2001, 2007a, and therein references). DM, HIMU, EMI and EMII mantle components, terrigenous and pelagic sediments, TS and PS, respectively (Zindler and Hart, 1986); crystalline basement (Comin-Chiaramontin et al., 1997). The $\varepsilon_t Sr$ and $\varepsilon_t Nd$ time-integrated values were calculated using the following values for Bulk Earth: $^{87}Sr/^{86}Sr$=0.7047; $^{87}Rb/^{86}Rb$=0.0827; $^{143}Nd/^{144}Nd$=0.512638; $^{147}Sm/^{144}Nd$=0.1967 (Faure, 2001). Paraguay array is according to Comin-Chiaramonti et al. (2007a, b and therein refereces).

Considering the whole Paraná-Agola-Etendeka system (PAE), and that the ASV is located at the central westernmost side of the PAE (Comin-Chiaramonti et al., 2007b, 2011 and therein references), the different geochemical behaviour in the different PAE sectors implies also different sources. Utilizing the T_{DM} (Nd) model ages (Gastal et al., 2005; Comin-Chiaramonti and Gomes, 2005), it should be noted that 1) the H-Ti flood tholeiites and dyke swarms from the Paraná Basin, and the Early Cretaceous potassic rocks and carbonatites from Eastern Paraguay range mainly from 0.9 to 2.1 Ga, whereas in Angola and Namibia the Early Cretaceous K-alkaline rocks vary from 0.4 to 0.9 Ga; 2) the L-Ti tholeiites display a major T_{DM} variation, from 0.7 to 2.4 Ga (mean 1.6±0.3) with an increase of the model ages from North to South; (3) Late Cretaceous alkaline rocks show model ages ranging from 0.6 to 1 Ga, similarly to the age span shown by the Triassic to Paleocene sodic alkaline rock-types lying along the Paraguay river (Comin-Chiaramonti, 2007a).

At any rate, the model ages seem indicate that some notional distinct "metasomatic events" may have occurred during Paleoproterozoic to Neoproterozoic times as precursor to the alkaline and tholeiitic magmas in the PAE (Comin-Chiaramonti and Gomes, 2005).

The meaning of model ages can be supported by another point of view. Considering that 1) the isotopic overlapping of different igneous rocks (i.e. tholeiites, alkaline rocks and carbonatites) cannot be accidental and points to sampling of ancient reservoirs formed at different times from the same subcontinental upper mantle (Carlson et al., 1996); 2) whatever the implication, i.e. heterogeneity induced by recycled crust in the mantle (Menzies, 1990; Weaver, 1991), or occurrence of variably veined material in the subcontinental upper mantle, or both (Foley, 1992a, b), Pb isotope data indicate a mantle source of ca. 1.8 Ga for the Paraná H-Ti tholeiites, and since much of the crust in southern Brazil appears to have been formed at ca. 2 Ga ago (Hawkesworth, 1986), it follows that magma genesis involved ancient lithospheric mantle reset at well defined isotopic ranges. A veined lithospheric mantle (amphibole/phlogopite-carbonate-lherzolite and amphibole-lherzolite+CO_2-fluid type III and IV veins of Meen et al. (1989) of Proterozoic age may well account for the magmatism both of the PAE and ASV (Fig. 8).
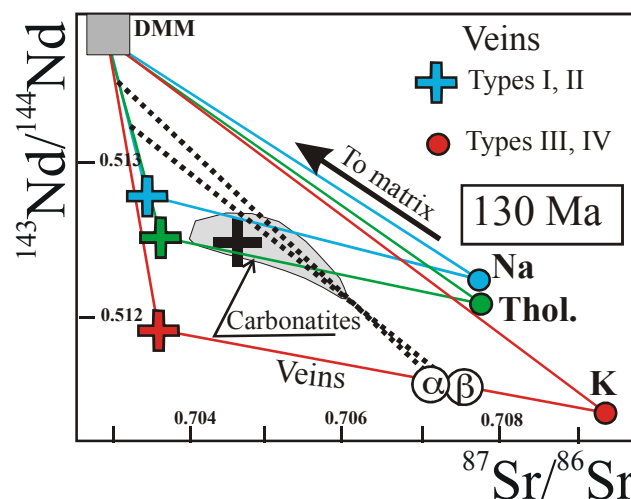
Fig. 8. Calculated subcontinental upper mantle (SCUM) isotopic composition at 2.0 Ga ago, projected to 130 Ma (Meen et al., 1989), modified after Fig. 10 of Comin-Chiaramonti et al. (2011). Parental melts with various Rb/Sr and Sm/Nd ratios are assumed for K , Na (potassic and sodic rocks from ASV, respectively: Comin-Chiaramonti et al., 1997) and PAE tholeiites (Piccirillo and Melfi, 1988). It should be noted that the compositions of metasomites formed from a single metasomatizing melt vary with the evolution of the melt. Consequently, the veins will define a trend of shallow slope, and mixing curves between vein and matrix will define an array towards the matrix (cf. a and b regression lines). Model depleted mantle (DMM): Rb=0, Sr=0.133, Sm=0.314, Nd=0.628; present day Bulk Earth: $^{87}Sr/^{86}Sr$=0.70475, $^{87}Rb/^{86}Sr$=0.0816, $^{143}Nd/^{144}Nd$=0.512638, $^{147}Sm/^{143}Nd$=0.1967; (Rb/Sr)$_{diopside}$: (Rb/Sr)$_{melt}$ ≈ 0.125, (Sm/Nd)$_{diopside}$: (Sm/Nd)$_{melt}$ ≈ 1.5; K: Rb/Sr=0.0957, Sm/Nd=0.1344; Na: Rb/Sr=0.0732, Sm/Nd=0.2295; Th: Rb/Sr=0.0733, Sm/Nd=0.2082.

In summary, the isotopic signature of the tholeiitic and K-Na- alkaline-magmatism from the PAE in general, and from ASV in particular, may reflect ancient heterogeneities preserved in the subcontinental lithospheric mantle. As matter of fact, all the data indicate that they represent a thermally-eroded metasomatic SCUM (subcontinental upper mantle) and/or delaminated lithospheric materials stored for long time, for example, towards the transition zone or deeper mantle in Archean-Proterozoic.

6. Geodynamic implications

General considerations to be made are largely based on the papers by Comin-Chiaramonti (1995, 2007a, b, c, d, 2011 and therein references). The geodynamic evolution of the ASV appears to be strictly linked to the evolution of the Western Gondwana (Fig. 1) that reflects the amalgamation processes which affected the region. The Western Gondwana geodynamic evolution at the Early Cretaceous requires an overall understanding of the pre-gondwanic situation, at least at the time of the Brasiliano cycle, both at the Atlantic and Pacific systems. The Brasiliano cycle was developed between about 890 to 480 Ma in a diachronic way, until the final arrangement of the framework basement of the South American Platform (Mantovani et al., 2005). The Gondwana amalgamation was achieved during Lower Ordovician: Unrug (1996) suggests a mosaic of lithospheric fragments linked by several (accretionary, collisional) Neo-Proterozoic mobile belts. After the amalgamation, the Gondwana supercontinent accumulated Paleozoic and Triassic-Jurassic sediments. Concomitantly, it was continuosly and laterally accreted to the western borders by means of successive orogenic belts, in the Lower Paleozoic and in the Permian-Triassic, until the Pangea formation (Cordani et al., 2000, 2005). The main cratonic fragments, descending from ancestors of the Pangea, were revorked, like the Amazonic and Rio de La Plata cratons and smaller ancient crustal blocks at the actual Paraguay boundaries (Kröner and Cordani, 2003). In this picture, the magmatism was driven by the relative extensional regimes derived by the relative movements of the ancient blocks (Fig. 9), probably induced by counterlockwise and clockwise movements (North and South, respectively) hinged at the about 20° and 24° South latitude (Prezzi and Alonso, 2002).

The geodynamic evolution of the ASV, Paraguay and neighbouring countries is apparent by the present day earthquake distribution along with the paleomagnetic, geological and geochemical evidences. The earthquake mechanisms (Berrocal and Fernandes, 1996) highlight the distribution of the earthquakes with hypocenters >500 km and <70 km, respectively (Fig. 9): the distribution of the deep earthquakes coincides with the inferred Nazca plate subduction at the Paraguay latitude (Fig. 10), where the depth of the lithospheric earthquakes, together with the paleomagnetic results (Ernesto et al., 1996; Randal, 1998; Rapolini, 2005), delineates different rotational paths at latitude of about 18-24°S (i.e. Chaco-Pantanal Basin). These data indicate extensional subplate tectonics at the Andean system (Randal, 1998) coupled with the lineaments of lithospheric earthquakes versus the Atlantic system that parallel the Ponta Grossa Arch and the lineaments of Rio Paraguay and Rio Pilcomayo, also clearly related to extensional environments (Berrocal and Fernandes, 1996; Comin-Chiaramonti and Gomes, 1996, 2005).

Also crucial to the the genesis of the ASV magma types is the link with the whole PAE system and with the geodynamic processes responsible for the opening of the South Atlantic. According to Nürberg and Müller (1991), the sea-floor spreading in the South Atlantic at ASV latitude started at about 125-127 Ma (Chron M4), but at north of the Walvis-Rio Grande ridge (Fig. 1B) the onset of the oceanic crust would be younger, e.g. 113 Ma (cf. Chang et al., 1988). In this context, the Early Cretaceous alkaline (and alkaline-carbonatite) complexes from ASV (and PAE) are subcoeval with respect to the main flood tholeiites of the Paraná Basin and, therefore, occurred during the early stages of rifting, before the main continental separation.
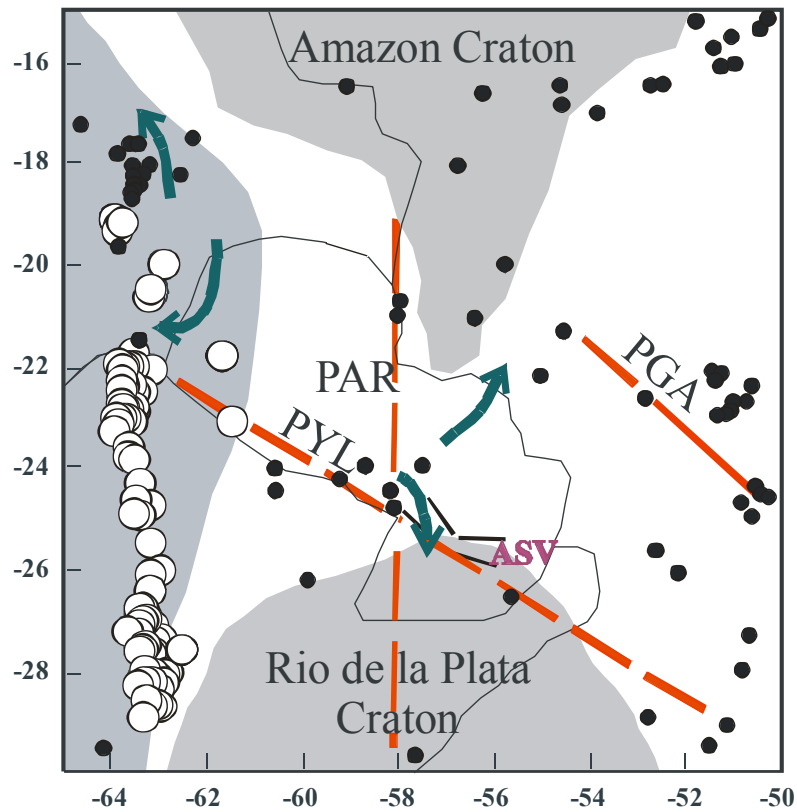
Fig. 9. Earthquakes distribution at the Paraguay and neighbouring regions: open and full circles, earthquake hypocenters >500 and <70 km, respectively (Berrocal and Fernandes, 1996). Red lines indicate extensional lineaments: PGA, Ponta Grossa Arch; PAR and PYL, Paraguay and Pylcomaio lineaments, respectively (cf. also inset of Fig. 3). The sky-blue lines delineate the rotational subplate trends (Comin-Chiaramonti and Gomes, 1996; Randall, 1998). ASV: Asunción-Sapucai-Villarrica graben.
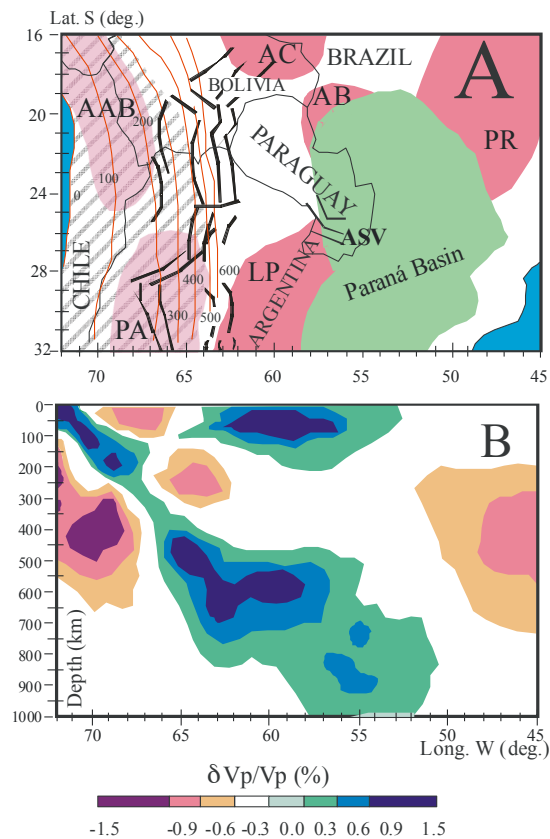
Fig. 10. A: General map, including ASV, showing contours (red lines) of the depth (km) of the subducting Nazca slab based on seismic data of [104]. Heavy lines (black) outline the Cretaceous rift systems. The hatched area roughly marks the extension of intense early Paleozoic reworking of Proterozoic material, but the exact border to the Brazilian Craton remains unknown [105]. Pink fields delineate inferred positions of major cratonic fragments below Phanerozoic cover [106]: AAB, Arequipa-Antofalla; AC, Amazon Craton; AB, Apa Block; PR, Paranapanema; LP, Rio de la Plata; PA, Pampia.

B: Seismic tomography image [107] across a profile approximately at 24° Lat. S. Note that the low-velocity feature in the mantle to the East has been interpreted as a fossil mantle plume by [108; cf. 109].

Also crucial to the the genesis of the ASV magmas types is the link with the whole PAE system and with the geodynamic processes that promoted the opening of the South Atlantic. According to [110] the sea-floor spreading in the South Atlantic at ASV latitude started at about 125-127 Ma (Chron M4), but north of the Walvis-Rio Grande ridges (cf. Fig. 1B) the onset of the oceanic crust would be younger, e.g. 113 Ma [111]. In this context the Early Cretaceous alkaline (and alkaline-carbonatite) complexes from ASV (and PAE) are subcoeval with respect to the main flood tholeiites of the Paraná Basin and, therefore, occurred during the early stages of rifting, before the main continental separation.

The origin of alkaline-carbonatitic magmatism in terms of plate tectonics is currently debated [31, 41]. Notably, the different westward angular velocity of the lithospheric fragments in the South American plate, as defined by the "second order plate boundaries" , e.g. the Pylcomaio lineament [112], as well as the different rotational trends at S19-24° Latitude, may favour the decompression and melting at different times of variously metasomatized (wet spot) portion of the lithospheric mantle with variable isotopic signatures [19, 79]. Small-scale metasomatism is suggested by the different suites of mantle xenoliths and significant H-O-C and F are also expected in the mantle source from the occurrence of the related carbonatites. The latter imply a lowering of the solidus, and along with an extensional tectonic, favour the melting of the mantle and magma ascent. This scenario also accounts for the presence of Late Cretaceous to Tertiary sodic magmatism in the PAE and in the Eastern Paraguay, where rifting structures are apparent (cf. Figs. 2 and 4).

Concluding remarks

Geological and geophysical evidences show that the Mesozoic-Tertiary block faulting tectonics in Eastern Paraguay is responsible for NW-trending grabens (ASV and Amambay), fault systems and fault-controlled basins, e.g. Jejui-Aguaray-Guazu, Asunción-Encarnación, San Pedro (cf. Fig. 2).

Distinct magmatic events are widespread in the Asunción-Sapucai-Villarrica graben, the major extensional structure in Eastern Paraguay, i.e. Early Cretaceous tholeiites and K-alkaline-carbonatitic complexes and dykes, along with Tertiary sodic magmatism. It is expected that beneath a rifted continental area, as ASV, the lithospheric mantle may have been thinned and subjected to high heat flow. This allowed the geotherm to intersect the peridotite solidus in the presence of H_2O-CO_2 rich fluids. Under these conditions, asthenospheric-derived melts may form, dissolving most of the "volatile" phases and, by percolating through a porous and deformed rock matrix, invaded the base of the lithosphere and favoured metasomatic processes at different levels in the peridotitic lithosphere with the formation of amphibole and/or phlogopite ("veined mantle" of [92]). Notably, the different tholeiitic (high- and low-Ti), K-alkaline suites (B-P and Ab-T) and sodic magmatism with HK and LK xenoliths are consistent with variously depleted lithosperic mantle at different times, pervasively and locally invaded by metasomatizing fluids and/or melts [112]. Thereafter , the newly formed veins ("enriched component") and peridotitic matrix ("depleted component") untervent different isotopic compositions with time, depending on their parent/daughter ratio (cf, Fig. 8), testifying to heterogeneous mantle sources beneath ASV.

Acknowledgments

References

ANSCHUTZ Co. 1981. Geologic Map of Eastern Paraguay (1:500,000), WIENS compiler. Denver, Colorado.

ANTONINI P., GASPARON M., COMIN-CHIARAMONTI P. AND GOMES C.B. 2005. Post-Palaeozoic magmatism in Eastern Paraguay: Sr-Nd-Pb isotope compositions. In: COMIN-CHIARAMONTI P. AND GOMES C.B. (Eds.) Mesozoic to Cenozoic Alkaline Magmatism in the Brazilian Platform. Edusp-Fapesp-SãoPaulo-Brazil, p. 57-70.

BELLIENI G., COMIN-CHIARAMONTI P., MARQUES L.S., MELFI A.J., PICCIRILLO E.M., NARDI A.J.R. AND ROISEMBERG A. 1984. High- and low-TiO_2 flood basalts of Paraná plateau (Brazil): petrology, petrogenetic aspects and mantle source relationships. N.Jb.Min.Abh., 150: 273-306.

BELLIENI G., COMIN-CHIARAMONTI P., MARQUES L.S., MARTINEZ L.A., MELFI A.J., NARDI A..J. R. AND PICCIRILLO E.M. 1986a. Continental flood basalts from the central-western regions of the Paraná plateau (Paraguay and Argentina): petrology and petrogenetic aspects. Neues Jahrbuch für Mineralogie Abh. 154: 111-139.

BELLIENI G., COMIN-CHIARAMONTI P., MARQUES L.S., MELFI A.J., PICCIRILLO E.M., NARDI A.J.R., PAPATRECHAS C., ROISEMBERG A. AND STOLFA D. 1986b. Petrogenetic aspects of acid and basaltic lavas from the Paraná plateau (Brazil): geological, mineralogical and petrochemical relationships. Journal of Petrology, 27: 915-944.

BERROCAL J. AND FERNANDES C. 1996. Seismicity in Paraguay and neighbouring regions. In: COMIN-CHIARAMONTI P. AND GOMES C.B. (Eds.) Alkaline magmatism in Central-Eastern Paraguay, Relationships with coevalmagmatism in Brazil. Edusp/Fapesp, São Paulo, Brazil, p. 57-66.

CARLSON R.W., ESPERANÇA S. AND SVISERO D.P. 1996. Chemical and Os isotopic study of Cretaceous potassic rocks from southern Brazil", Contrib. Mineral. Petrol., 125: 393-405.

CASTORINA F., CENSI P., COMIN-CHIARAMONTI P.,PICCIRILLO E.M., ALCOVER NETO F., GOMES C.B., RIBEIRO DE ALMEIDA T., SPEZIALE S. AND TOLEDO C.M. 1997. Carbonatites from Eastern Paraguay and genetic relationshipss with potassic magmatism: C, O, Sr and Nd isotopes. Mineralogy and Petrology, 61: 237-260.

CHANG H.K., KOWSMANN R.O. AND FIGUEREIDO de A.M.F. 1988. New concept on the development of east Brazilian margin basins. Episodes, 11: 194-202.

CHIBA H., CHACK T., CLAYTON R.N. AND GOLDSMITH J. 1989. Oxygen isotope fractionations involving diopside, forsterite, magnetite, and calcite: application to geothermometry. Geochimica et Cosmochimica Acta, 53: 2985-2995.

COMIN-CHIARAMONTI P. AND GOMES C.B. (Eds.). 1996. Alkaline Magmatism in Central-Eastern Paraguay. Relationships with coeval magmatism in Brazil. São Paulo, Brazil, Edusp/Fapesp, 464 p.

COMIN-CHIARAMONTI P. AND GOMES C.B. (Eds.). 2005. Mesozoic to Cenozoic Alkaline Magmatism in the Brazilian Platform, Edusp/Fapesp, São Paulo, Brazil, 757 p.

COMIN-CHIARAMONTI P., GOMES C.B., DE MIN A., MELFI A.J., BELLIENI G., CASTILLO A.M., VELAZQUEZ J.C., VELAZQUEZ V.F. AND PICCIRILLO E.M. 1989. Atividade filoniana asociada ao complexo alcalino de Sapukai, Paraguay Oriental. Geochim. Brasiliensis, 3: 93-114.

COMIN-CHIARAMONTI P., CUNDARI A., GOMES C.B., PICCIRILLO E.M., BELLIENI G., CENSI P., DEMIN A., ORUÉ D. AND VELAZQUEZ V.F.1990. Mineral chemistry and its genetic significance of major and accessory minerals from a potassic dyke swarm in the Sapucai graben, Central-Eastern Paraguay. Geochim.Brasil., 4: 175-206.

COMIN-CHIARAMONTI P., CIVETTA L., PICCIRILLO E.M., BELLIENI G., BITTSCHENE P., DEMARCHI G., GOMES C.B., CENSI P., PETRINI R., CASTILLO A.M.C. AND VELÁZQUEZ J.C. 1991. Tertiary nephelinitic magmatism in Eastern Paraguay: petrology, Sr-Nd isotopes and genetic relationships with associated spinel-peridotite xenoliths. Europ. Journ.Mineral., 3: 507-525.

COMIN-CHIARAMONTI P., CUNDARI A., GOMES C.B., PICCIRILLO E.M., CENSI P., DEMIN A., BELLIENI G., VELÁZQUEZ V.F. AND ORUÈ, D. 1992a. Potassic dyke swarm in the Sapucai graben, Eastern Paraguay: petrographical, mineralogical and geochemical outlines. Lithos, 28: 283-301.

COMIN-CHIARAMONTI P., CENSI P., CUNDARI A AND GOMES C.B. 1992b. A silico-beforsitic flow from the Sapucai Complex (Central-Eastern Paraguay). Geochim. Brasiliensis, 6: 87-92.

COMIN-CHIARAMONTI P., GOMES C.B., CENSI P., DEMIN A., ROTOLO S., VELAZQUEZ V.F. 1993. Geoquimica do magmatismo Post-Paleozoico no Paraguai Centro-Oriental. Geochim. Brasiliensis, 7: 19-34.

COMIN-CHIARAMONTI P., CASTORINA F., CUNDARI A., PETRINI R., GOMES C.B. 1995. Dykes and sills from Eastern Paraguay: Sr and Nd isotope systematic. In:Baer G. and Heiman A. (Eds.) IDC-3, Physics and Chemistry of Dykes, Balkema, Rotterdam, p. 267-278.

COMIN-CHIARAMONTI P., DE MIN A. AND GOMES C.B. 1996a. Magmatic rock-types from the Asunción-Sapucai graben: descrption of the occurrences and petrographical notes. In: COMIN-CHIARAMONTI P. AND GOMES C.B. (Eds.) Alkaline Magmatism in Central-Eastern Paraguay. Relationships with Coeval Magmatism in Brazil, Edusp-Fapesp, São Paulo, Brazil, p. 275-330.

COMIN-CHIARAMONTI P., DE MIN A. AND MARZOLI A. 1996b. Magmatic rock-types from the Asunción-Sapucai graben: chemical analyses. In: COMIN-CHIARAMONTI P. AND GOMES C.B. (Eds.) Alkaline Magmatism in Central-Eastern Paraguay. Relationships with Coeval Magmatism in Brazil, Edusp-Fapesp, São Paulo, Brazil, p. 331-387.

COMIN-CHIARAMONTI P., CUNDARI A., BELLIENI G. 1996c. Mineral analyses of alkaline rock-types from the Asunción-Sapucai graben. In: COMIN-CHIARAMONTI P. AND GOMES C.B. (Eds.) Alkaline Magmatism in Central-Eastern Paraguay. Relationships with Coeval Magmatism in Brazil, Edusp-Fapesp, São Paulo, Brazil, p. 389-458.

COMIN-CHIARAMONTI P., CUNDARI A., DE MIN A., GOMES C.B. AND VELÁZQUEZ V.F. 1996d. Magmatism in Eastern Paraguay: occurrence and petrography. In: COMIN-CHIARAMONTI P. AND GOMES C.B. (Eds.) Alkaline Magmatism in Central-Eastern Paraguay. Relationships with Coeval Magmatism in Brazil. Edusp-Fapesp, São Paulo, Brazil, p. 103–122.

COMIN-CHIARAMONTI P., CUNDARI A., PICCIRILLO E.M., GOMES C.B., CASTORINA F., CENSI P., DEMIN A., MARZOLI A., PETRINI R. AND SPEZIALE S. 1997. Potassic and sodic igneous rocks from Eastern Paraguay: their origin from the lithospheric mantle and genetic relationships with the associated Paraná flood tholeiites. Journal of Petrology, 34: 495-528.

COMIN-CHIARAMONTI P., CUNDARI A., DE GRAFF J.M., GOMES C.B. AND PICCIRILLO E.M. 1999. Early Cretaceous-Tertiary magmatism in Eastern Paraguay (western Paraná basin): geological, geophysical and geochemical relationships. Journal of Geodynamic*s*, 28: 375-391.

COMIN-CHIARAMONTI P., PRINCIVALLE F., GIRARDI V.A.V., GOMES C.B., LAURORA A. AND ZANETTI R. 2001. Mantle xenoliths from Ñemby, Eastern Paraguay: O-Sr-Nd isotopes, trace elements and crystal chemistry of hosted clinopyroxenes. Periodico di Mineralogia, 70: 205-230.

COMIN-CHIARAMONTI P., MARZOLI A., GOMES C. B., MILAN A., RICCOMINI C., MANTOVANI M.M.S., RENNE, P., TASSINARI C.C.G. AND VASCONCELOS, P.M. 2007a. Origin of Post Paleozoic Magmatism in Eastern Paraguay. In: FOULGER G.R.AND JURDY D.M. (Eds.), P^4 Book, The Geological Society of America, Special Paper 430, p. 603-633.

COMIN-CHIARAMONTI P., GOMES C. B., ERNESTO M., MARZOLI A. AND RICCOMINI C. 2007b. Eastern Paraguay: Post-Paleozoic Magmatism. In: Large Igneous Province of the month, January 2007. http://www.largeigneousprovinces.org/links.html, 29 p.

COMIN-CHIARAMONTI P., GOMES C.B., CUNDARI A., CASTORINA F. AND CENSI P. 2007c. A review of carbonatitic magmatism in the Paraná-Angola-Etendeka (Pan) System. Periodico di Mineralogia., 76: 25-78.

COMIN-CHIARAMONTI P., MARZOLI A., GOMES C.B., MILAN A., RICCOMINI R. MANTOVANI M.M.S., RENNE, P., TASSINARI C.C.G., VASCONCELOS, P.M. 2007d. Origin of Post Paleozoic Magmatism in Eastern Paraguay. In: FOULGER G.R. AND JURDY, D.M. (Eds.) P^4 Book, The Geological Society of America, Special Paper, 430, p. 603-633.

COMIN-CHIARAMONTI P., LUCASSEN F., GIRARDI V.A.V., DE MIN A. AND GOMES C.B. 2009. Lavas and their mantle xenoliths from intracratonic Eastern Paraguay (South American Platform) and Andean Domain, NW-Argentina: a comparative review. Mineralogy and Petrology, 98: 143-165.

COMIN-CHIARAMONTI P., DE MIN A., GIRARDI V.A.V. AND RUBERTI E. 2011. Post-Paleozoic magmatism in Angola and Namibia: a review. In: BECCALUVA L., BIANCHINI G. AND WILSON M. (Eds), Volcanism and evolution of the African lithosphere. Geological Society of America, Special .Paper 478, p. 223-247.

CORDANI U.G., SATO K., TEIXEIRA W., TASSINARI C.C.G. AND BASEI M.A.S. 2000. Crustal evolution of the South American platform. In: CORDANI U.G., MILANI E.J., THOMAZ FILHO A.A. AND CAMPOS D.A. (Eds) Tectonic Evolution of South America. 31st International Geological Congress, Rio de Janeiro, p. 19-40.

CORDANI U.G., TASSINARI C.C.G., AND ROLIM D.R. 2005. The basement of the Rio Apa Craton in Mato Grosso do Sul (Brazil) and northern Paraguay: a geochronological correlation with the tectonic provinces of the south-western Amazonian Craton. Gondwana Conference, Abstracts volume, Mendoza, Argentina, p. 1-12.

CUNDARI A. AND FERGUSON A.K. 1982. Significance of the Pyroxene chemistry in leucite-bearing and related assemblages. Tchermaks Mineral. Petrogr. Mitt., 30: 189-204.

DE GRAFF, J.M. 1985. Late Mesozoic crustal extension and rifting on the western edge of the Paraná Basin, Paraguay", Geological Society of America, Abstracts with Programs, 17: p. 560.

DE GRAFF J.M., GAY S.P. Jr. AND ORUÉ D. 1981. Interpretación geofísica and geológica del Valle de Ypacaraí (Paraguay) y su formación. Revista de la Asociación Geológica Argentina, 36: 240-256.

de La ROCHE H. 1986 Classification and nomenclature des roches ignées: un essai de restauration de la convergence entre systématique quantitative, typologie d'usage et modélisation génétique. Bulletin de la Societé Geologique de France, 8: 337-353.

DE MARCHI G., COMIN-CHIARAMONTI P., DEVITO P., SINIGOI S. AND CASTILLO A.C.C. 1988. Lherzolite-dunite xenoliths from Eastern Paraguay: petrological constraints to mantle metasomatism. In: PICCIRILLO E.M. AND MELFI A.J. (Eds.) T*he* Mesozoic flood volcanism of the Paranà basin: petrogenetic and geophysical aspects. IAG, Sao Paulo, Brazil, p. 207-228.

DRUECKER M.D. AND GAY S.P. Jr. 1987. Mafic dyke swarms associated with Mesozoic rifting in Eastern Paraguay, South America. In: HALLS H.C. AND A.R. FAHRIG A.R. (Eds), Mafic dyke swarms, Geological Association of Canada, Sp.P. p 187-193.

EDGAR A.D. 1980. Role of subduction on the genesis of leucite-bearing rocks: a discussion. Contrib. Mineral. Petrol., 73: 429-431.

ERLANK A. J., WATERS F. G., HAWKESWORTH C. J., HAGGERTY S. E., ALLSOPP H. L., RICKARD R. S. AND MENZIES M.A. 1987. Evidence for mantle metasomatism in peridotite nodules from the Kimberley pipes, South Africa. In: MENZIES M.A. AND HAWKESWORTH C. J. (Eds) Mantle Metasomatism. London, Academic Press, p. 221–309

ERNESTO M., COMIN-CHIARAMONTI P., GOMES C.B., CASTILLO A.M.C. AND VELAZQUEZ V.F. 1996. Palaeomagnetic data from the central alkaline province, Eastern Paraguay. In: COMIN-CHIARAMONTI P. AND GOMES C.B. (Eds.) Alkaline Magmatism in Central-Eastern Paraguay. Relationships with Coeval Magmatism in Brazil, Edusp-Fapesp, São Paulo, Brazil, p. 85-102.

FABRIÈS J. 1979. Spinel-olivine geothermometry in peridotites from ultramafic complexes. Contrib. Mineral. Petrol., 69: 329-336.

FAIRHEAD J.D. AND WILSON M. 2005. Plate tectonic processes in the South Atlantic Ocean: do we need mantle plumes? In: FOULGER G.R., NATLAND J.H., PRESNALL D.C. AND D.L. ANDERSON (Eds), Plates, Plumes and Paradigms, The Geological Society of America, Special Paper, 388, p. 537-553.

FAURE G. 2001. Origin of igneous rocks: The isotopic evidence", Berlin, Springer, 496 p..

FENG M., LEE V.D.S. AND ASSUMPÇÃO M. 2007. Upper mantle srructure of South America from joint inversions of waveforms and fundamental mode group velocities of Rayleigh waves. Journal of Geophysical Research, 112: 1-16.

FOLEY S.F. 1992. Petrological characterization of the source components of potassic magmas: geochemical and experimental constraints. Lithos, 28: 187-204.

FOLEY S.F. 1992. Vein plus wall-rock melting mechanism in the lithosphere and origin of potassic alkaline magmas. Lithos, 28: 435-453.

FREY F.A. AND GREEN D.H. 1979. The mineralogy, geochemistry and origin of lherzolite inclusions in Victorian basante. Geochim. Cosmochim: Acta, 38: 1023-1050.

GASTAL M.P., LAFON J.M., HARTMANN L.A. AND KOESTER E. 2005. Sm-Nd isotopic investigation of Neoproterozoic and Cretaceous igneous rocks from southern Brazil: a study of magmatic processes. Lithos, 82: 345-377.

GREEN P.F., DUDDY I.R., O'SULLIVAN P., HEGARTY K.A., COMIN-CHIARAMONTI P**.,** GOMES C.B. 1991. Mesozoic potassic magmatism from the Asunción-Sapucai graben: apatite fission track analysis of the Acahai suite and implication for hydrocarbon exploration", Geochim.Brasil., 5: 79-88.

GUDMUNDSSON O. AND SAMBRIDGE, M. 1998. A regionalized upper mantle (RUM) seismic model. Journal of Geophysical Research., 103: 7121-7136.

HART S.R. AND ZINDLER A. 1989. Constraints on the nature and the development of chemical heterogeneities in the mantle. In:PELTIER W.R. (Ed.) Mantle convection plate tectonics and global dynamics. New York: Gordon and Breach Sciences Publishers, p. 261-388.

HAWKESWORTH C.J., GALLAGHER K., KELLEY S., MANTOVANI M., PEATE D.W., REGELOUS M. AND ROGERS N.W. 1992. Paraná magmatism and the opening of the South Atlantic. In: Storey B.C. (Ed.). Magmatism and the Causes of Continental Break-up. Geological Society of London Sp. P., 68, p. 221–240.

HAWKESWORTH C.J., MANTOVANI M.S.M., TAYLOR P.N. AND PALACZ Z. 1986. Evidence from the Paraná of south Brazil for a continental contribution to Dupal basalts. Nature, 322: 356-359.

HEGARTY K. L., DUDDY I.R. AND GREEN P.F. 1996. The thermal history in around the Paraná basin using apatite fission track analysis—implications for hydrocarbon occurrences and basin formation. In: COMIN-CHIARAMONTI P. AND GOMES C.B. (Eds*.)* Alkaline magmatism in Central-Eastern Paraguay, Relationships with coevalmagmatism in Brazil. Edusp/Fapesp, São Paulo, Brazil, p. 67–84.

HUTCHINSON D.S. 1979. Geology of the Apa High. TAC, Internal Report, Asunción: 46 p.

KANZLER A. 1987. The southern Precambrian in Paraguay. Geological inventory and age relations. Zentralblatt f*ür* Geologie und Paläontologie, 7: 753-765.

KRÖNER A. AND CORDANI U.G. 2003.African, southern India and South American cratons were not part of the Rodinia supercontinent: evidence for field relationships and geochronology. Tectonophysics, 375: 325-352.

KYSER, T.K. 1990. Stable isotopes in the continental lithospheric mantle: In: MENZIES M.A. (Ed.). Continental mantle, Oxford Clarendon Press, p. 127-156.

KYSER T.K., J.R. O'NEIL J.R. AND CARMICHAEL I.S.E. 1981. Oxygen isotope thermometry of basic lavas and mantle nodules. Contrib. Mineral. Petrol., 77: 11-23.

LAUX J.H., PIMENTEL M.M., DANTAS E.L., JUNGES S.L. AND ARMSTRONG R 2005. Two Neoproterozoic crustal accretion events in the Brasilia belt, central Brazil. Journal of South American Earth Sciences, 18: 183-198.

LE MAITRE R.P. 1989. A Classification of Igneous rocks and Glossary of Terms. Oxford, Blackwell, 193 p.

LIU H.K., GAO S.S., SILVER P.G. AND ZHANG Y. 2003. Mantle layering across central South America. Journal of Geophysical Research, 108, B11: 2510.

LIVIERES R.A. AND QUADE H. 1987. Distribución regional y asentamiento tectónico de los complejos alcalinos del Paraguay, Zentralblatt für Geologie und Paläontologie, 7: 791-805.

LUCASSEN F., BECCHIO R., WILKE H.G. THIRWALL, M.F.; VIRAMONTE, J.; FRANZ, G. AND WEMMER, K. 2000. Proterozoic- Paleozoic development of the basement of the Central Andes (18°-26°) – a mobile belt of the South American craton. Journal of South American Earth Sciences, 13: 697-715.

MANTOVANI M.S.M., QUINTAS M.C.L., SHUKOWSKY W. AND BRITO NEVES B.B. 2005. Delimitation of the Paranapanema Proterozoic block: a geophysical contribution. Episodes, 28: 18-22.

MATTEY D., LOWRY D. AND MACPHERSON C. 1994. Oxygen isotope composition of mantle olivine. Earth and Planetary Science Letters, 128: 231-241.

MCKENZIE D.P. AND O'NIONS M.J. 1995. The source regions of ocean island basalts. Journal of Petrology, 36: 133-159.

MEEN J.K., AYERS J.C. AND FREGEAU E.J. 1989. A model of mantle metasomatism by carbonated alkaline melts: trace element and isotopic compositions of mantle source regions of carbonatite and other continental igneous roks. In: BELL K. (Ed.) Carbonatites, genesis and evolution. London, Unwin Hyman, p. 464-499

MENZIES M.A. (Ed.). 1990 Continental mantle. Oxford Clarendon Press, 450 p.

MENZIES M.A. AND C.J. HAWKESWORTH C.J. (Eds.). 1987. Mantle metasomatism. Academic press, Geology Series, 453 p.

MENZIES M.A. AND WASS S.Y. 1983. CO_2 and LREE-rich mantle below eastern Australia; a REE and isotopic study of alkaline magmas and apatite-rich mantle xenoliths from the Southern Highlands Province, Australia. *Earth and Planetary Science Letters,* 65: 287-302.

MERCIER J.C. 1980. Single-pyroxene geothermometry and geobarometry. American Journal of Sciences, 61: 603-615.

MERCIER J.C., BENOIT V. AND GIRARDEAU J. 1984. Equilibrium state of diopside-bearing harzburgites from ophiolites: geobarometric and geodynamic implications. Contrib. Mineral. Petrol., 85: 391-403.

NÜRBERG D. AND MÜLLER R.D. 1991. The tectonic evolution of South Atlantic from Late Jurassic to present. Tectonophysics, 191: 27-43.

O'REILLY S.Y., AND GRIFFIN W.C. 1988. Mantle metasomatism beneath western Victoria, Australia. 1: Metasomatic processes in Cr diopside lherzolites" Geochimica et Cosmochimica Acta, 52: 433-448.

PHOTO GRAVITY Co. 1991 Regional Bouguer Gravity data and station location Map of the Paraguay (Scale 1: 2,000,000), Asunción, Archivo DRM-MOPC.

RENNE P.R., DECKART K., ERNESTO M., FÉRAUD G. AND PICCIRILLO E.M. 1996. Age of the Ponta Grossa dike swarm (Brazil), and implications to Paraná flood volcanism. Earth and Planetary Science Letters, 144: 199–211, 1996.

RENNE P.R., ERNESTO M., PACCA I.G., CO, R.S., GLEN J., PREVOT M., AND PERRIN M. 1992. The age of Paraná flood volcanism, rifting of Gondwanaland, and the Jurassic-Cretaceous boundary. Science, 258: 975–979.

RENNE P.R., MERTZ D.F., TEIXEIRA W., ENS H. AND RICHARDS M. 1993. Geochronologic constraints on magmatic and tectonic evolution of the Paraná Province. American Geophysical Union Abstract, 74: 553, 1993.

PEATE D.W. 1992. The Parana-Etendeka Province. In: MAHONEY J. AND COFFIN, M.F. (Eds.) Large Igneuos Province: Continetal, Oceanic, Planetary Flood Volcanism,. American Geophyscial Union, Washington, DC, USA, p. 217–245.

PEATE D.W. AND HAWKESWORTH C.J. 1996. Lithospheric to asthenospheric transition in low-Ti flood basalts from Southern Paraná, Brazil. Chemical Geology, 127: 1-24.

PERKINS G., ZACHARY S., AND SERVERSTONE J. 2006. Oxygen isotope evidence for subduction and rift-related mantle metasomatism beneath the Colorado Plateau-Rio Grande rift transition. Contrib. Mineral. Petrol.,151: 633-650.

PICCIRILLO E.M. AND MELFI A.J. (Eds,). 1988. T*he* Mesozoic flood volcanism of the Paranà basin: petrogenetic and geophysical aspects. IAG, Sao Paulo, Brazil, 600 p.

PICCIRILLO E.M., BELLIENI G., COMIN-CHIARAMONTI P., ERNESTO M., MARQUES L., NARDI A.J.R., PACCA I.G., ROISEMBERG A. AND STOLFA D. 1988. Continental flood volcanism from the Parana' Basin (Brazil). In: MCDOUGAL J.D. (Ed.) Continental flood volcanism. Kluver Acad. Publ., London, p. 195-238.

PICCIRILLO E.M., CIVETTA L., PETRINI R., LONGINELLI A., BELLIENI G., COMIN-CHIARAMONTI P., MARQUES L.S. AND MELFI A.J. 1989. Regional variations within the Paraná flood basalts (southern Brazil): evidence for subcontinental mantle, heterogeneity and crustal contamination. Chemical Geology, 75: 103-122.

PREZZI C.B. AND ALONSO R.N. 2002. New paleomagnetic data from the northern Argentina Puna: Central Andes rotation pattern reanalyzed. Journal of Geophysical Research, 107, B2: 1-18.

PRINCIVALLE F., TIRONE M. AND COMIN-CHIARAMONTI P. 2000. Clinopyroxenes from metasomatized spinel-peridotite mantle xenoliths from Ñemby (Paraguay): crystal chemistry and petrological implications. Mineralogy and Petrology, 70: 25-35.

RANDALL D.R. 1998. A New Jurassic-Recent apparent polar wander path for South America and a review of central Andean tectonic models. Tectonophysics, 299: 49-74.

RAPOLINI A.E. 2005. The accretionary history of Southern South America from latest Proterozoic to the Late Palaeozoic: some palaeomagnetic constraints. Geological Society, Sp. P., 246: 305-328.

RICCOMINI C., VELÁZQUEZ V.F. AND GOMES, C.B. 2001. Cenozoic lithospheric faulting in the Asunción Rift, Eastern Paraguay. Journal of South American Earth Sciences,. 14: 625-630.

RIVALENTI G., VANNUCCI R., RAMPONE E., MAZZUCCHELLI M., PICCARDO G.B., PICCIRILLO E.M., BOTTAZZI P. AND OTTOLINI L.. 1996. Peridotite clinopyroxene chemistry reflects mantle processes rather than continental versus oceanic settings. Earth and Planetary Science Letters, 139: 423-437.

RODEN M.F., FREY F.A. AND FRANCIS D.M. 1984. An example of consequent mantle metasomatism in peridotite inclusions from Nunivak Island, Alaska. Journal of Petrology, 25: 546-577.

ROGERS J.J.W., R. UNRUG R. AND M. SULTAN M. 1995. Tectonic assembly of Gondwana. Journal of Geodynamics. 19, 1-34.

SEN G., FREY F.A., SHIMIZU N. AND LEEMAN W.P. 1993. Evolution of the lithosphere beneath Oahu, Hawaii: rare earth element abundances in mantle xenoliths. Earth and Planetary Science Letters, 119: 53-69.

SPERA E.J. 1984. Carbon oxide in petrogenesis. III: role of volatiles in the ascent of alkaline-bearing magmas with special reference to xenolith-bearing mafic lavas. Contrib. Mineral. Petrol, 88: 217-232.

STRECKEISEN A. 1976. To each plutonic rock its proper name. Earth Science Reviews, 12: 1-33.

SUN S-S AND MCDONOUGH W.F. 1989. Chemical and isotopic systematics of oceanic basalts: implications for mantle composition and processes. In: SAUNDERS A.D. AND NORRY, M.J. (Eds), Magmatism in the Ocean Basins. Geological Society of London Sp. P., 42, p. 313-345.

TOMMASI A. AND VAUCHEZ A. 2001. Continental rifting parallel to ancient collisional belts: an effect of the mecanical anisotropy of the lithospheric mantle. Earth and Planetary Science Letters, 185: 199-210.

TURNER S., REGELOUS M., KELLEY S., HAWKESWORTH C.J. AND MANTOVANI M.S.M. 1994. Magmatism and continental break-up in the South Atlantic: high precision 40Ar-39Ar geochronology. Earth and Planetary Science Letters, 121: 333–348.

UNRUG R. 1996.The Assembly of Gondwanaland. Episodes, 19: 11-20.

UNTERNEHR P., CURIE D., OLIVET J.L., GOSLIN J. AND BEUZART P. 1988. South Atlantic fits and intraplate boundaries in Africa and South America. Tectonophysics, 155: 169-179.

USSAMI N., KOLISNYK A., RAPOSO MIB, FERREIRA F.J.F., MOLINA E.C. AND ERNESTO M. 1994. Detectabilidade magnetica de diques do Arco de Ponta Grossa: um estudo integrado de magnetometria terrestre/aerea e magnetismo de rocha. Revista Brasileira de Geociências, 21: .317-327.

VAN DECAR J.C., JAMES D. AND ASSUMPÇÃO M. 1995. Seismic evidence for a fossil mantle plume beneath South America and implications for driving forces. Nature, 378: 25-3.

VELÁZQUEZ V.F., C. GOMES C.B., RICCOMINI C., AND KIRK J. 2011. The Cretaceous Alkaline Dyke Swarm in the Central Segment of the Asunción Rift, Eastern Paraguay: its regional distribution, mechanism of emplacement, and tectonic significance. Journal of Geological Research, Article ID 946701: 18 p.

WANG J., HATTORI K.H., KILIAN R. AND STERN C.R. 2007. Metasomatism of sub-arc peridotites below southernmost South America: reduction of fO$_2$ by slab-melt. Contrib. Mineral. Petrol., 153: 607-624.

WEAVER B.L. 1991. The origin of ocean island basalt end-member compositions: trace element and isotopic constraints. Earth and Planetary Science Letters 104: 381-397.

WELLS PRA. 1977. Pyroxene thermometry in simple and complex systems. Contrib. Mineral. Petrol., 42: 109-121.

WIENS, F. 1982. Mapa geologica de la region oriental, Republica del Paraguay, escala 1:500,000. Simposio Recursos Naturales, Paraguay, Asunción: 9 p.

ZALAN P.V., WOLFF S., ASTOLFI M.A., SANTOS V.I., CONCEIÇÃO J.C., APPI V., NETO E.V.S., CERQUEIRA J.R. AND MARQUES A. 1990. The Paraná basin, Brazil. In: LEIGHTON M.W., KOLATA D.R., OLTTZ D.F. AND J.J. EIDEL J.J. (Eds) Interior cratonic basins. American Association of Petroleum Geology, Tulsa. Memoir, 51, p. 601-708.

ZINDLER A. AND HART S.R. 1986. Chemical geodynamics. Annual Review of Earth and Planetary Sciences, 14: 493-571.